E&G Quaternary Sci. J., 71, 1–22, 2022
https://doi.org/10.5194/egqsj-71-1-2022

Open Access E&G Quaternary Science Journal

Research article

Late Quaternary landform evolution and sedimentary successions in the Miaoli Tableland, northwestern Taiwan

Shih-Hung Liu, Robert Hebenstreit, and Margot Böse

Institute of Geographical Sciences, Department of Earth Sciences, Freie Universität Berlin, 12249 Berlin, Germany

Correspondence: Shih-Hung Liu (liushihhung@zedat.fu-berlin.de)

Relevant dates: Received: 28 April 2021 – Revised: 24 September 2021 – Accepted: 6 December 2021 – Published: 18 January 2022

How to cite: Liu, S.-H., Hebenstreit, R., and Böse, M.: Late Quaternary landform evolution and sedimentary successions in the Miaoli Tableland, northwestern Taiwan, E&G Quaternary Sci. J., 71, 1–22, https://doi.org/10.5194/egqsj-71-1-2022, 2022.

Abstract: Elevated Quaternary sedimentary complexes in the western foreland of the central mountain ranges of Taiwan are called tablelands. Their mostly flat surfaces are deeply incised by fluvial processes. The landforms and the fluvial systems in the Miaoli Tableland are investigated by high-resolution terrain analyses based on different datasets. Sediments are described in 51 outcrops and characterized by grain size composition. The outcrops revealed complete or incomplete sequences of the general scheme from bottom to top: sandy tidal–coastal units overlain by gravel- and cobble-rich fluvial deposits always with a fine-grained silt-rich top cover layer influenced by aeolian deposits. All layers are unconsolidated sediments. Three subtypes of this sequence were identified, with respect to the occurrence of the fluvial deposits. The relation of tectonic and erosional processes including the rework of gravels is discussed. The results reveal a tableland surface much more disaggregated than previously mapped, suggesting that individual tableland segments represent remnants of an inferred palaeotopography. The tableland surfaces have been separated into Sedimentary Highlands (SH-I and SH-II) and Sedimentary Terraces (ST) by geometrical properties. The Alluvial and Coastal Plains (AL) represent broad valley bottoms ("box-shaped valleys") in the dendritic drainage systems below 150 m and the coastal plains. The landforms and predominantly the sediment sequences are discussed in the context of the existing stratigraphical schemes of the Toukoshan Formation and the so far rarely used Lungkang Formation. The latter is recommended as the stratigraphical term for the refined subdivision of the uppermost part of late Quaternary sediments in the Miaoli Tableland.

1 Introduction

Sedimentary terraces are landforms which are formed by deposition, base level change, and subsequent erosion. They provide stratigraphic records and represent archives for changes in sedimentary and erosional processes (Charlton, 2008). The process-inducing environmental factors are climate change, sea-level change, and local tectonism, which have been studied in various regions worldwide for interpreting the landscape evolution of sedimentary terraces (e.g. Bridgland and Westaway, 2008; Robustelli et al., 2014; Pickering et al., 2014; Mather et al., 2017).

Huge sedimentary complexes are distributed in the western foreland of the Taiwanese mountain ranges (Yu and Chou, 2001; Yang et al., 2006) (Fig. 1a). They are dissected by fluvial incision, thus forming terraces, which are called

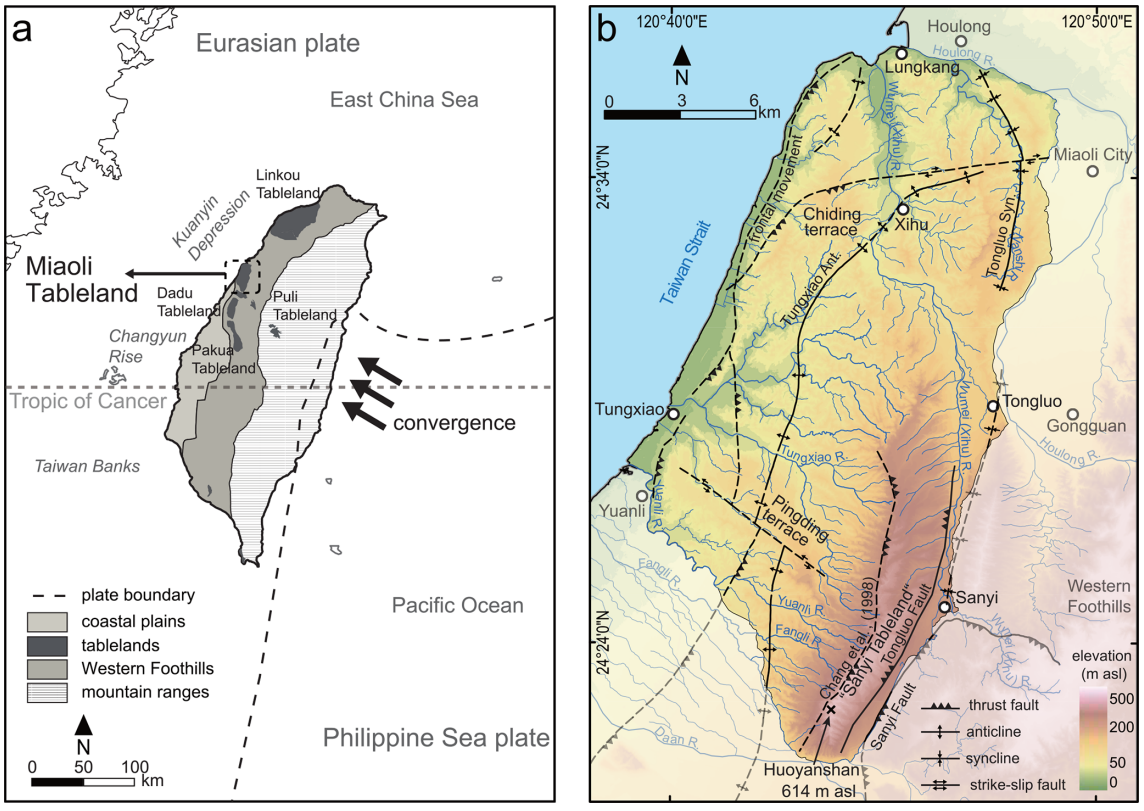

Figure 1. Location of the Miaoli Tableland and other tablelands in Taiwan. Generalized tectonic context after Angelier et al. (1986) and Suppe (1984); geological divisions modified after Ho (1988). **(b)** Detail map of the study area. Elevation extracted from an open-access digital elevation model (DEM) with 20 m resolution (Satellite Survey Center, 2018); tectonic features adapted from geological maps (Central Geological Survey, 2017); locations of the Tongluo Fault and name of "Sanyi Tableland" by Ota et al. (2006).

"tablelands" by local scientists (Lin, 1957; Teng, 1979; Lin and Chou, 1978; Tomita, 1954; Chang et al., 1998; Tsai et al., 2006, 2010). Landforms similar to the tablelands have been described in the western Pacific area, such as in Japan (Matsu'ura et al., 2014) and Korea (Choi et al., 2009).

However, until now, the detailed formation history of these sedimentary terraces has been widely unclear, even though detailed studies focused on different aspects of the tableland morphology such as the local tectonism (Shyu et al., 2005; Yang et al., 2006; Shih and Yang, 1985), the long-term sedimentation since the Neogene (Teng, 1996b; Teng et al., 2001), or weathering degrees and their corresponding relative chronology of the surface materials (Ota et al., 2002; Shih and Yang, 1985; Tsai et al., 2006). The majority of these studies follow the interpretations that, according to the continuous tectonic uplift since the Pliocene, the age of the tablelands' sedimentary units ranges from the Pliocene to early Pleistocene (Chang, 1953). Only a few studies included or focused on the late Quaternary sedimentation and surface morphology of the tablelands (Ota et al., 2006; Tseng et al., 2013; Horng, 2014; Chang et al., 1998; Teng et al., 2001; Siame et al., 2012).

The sedimentary sequences represent potentially valuable archives of the Quaternary landscape history of western Taiwan. As the mountainous island is located in a unique position at the Tropic of Cancer between the Asian continent and the western Pacific, these archives may even have implications for the entire region in terms of palaeoclimate and sea-level change. Thus, more detailed morphological studies are required in order to understand the complicated nature of these terraces on the basis of a reconstruction of the process history. This study presents – as a first step – an approach for interpreting morphological processes by the combination of a concise 3D terrain analysis and sedimentological studies by field observation and particle size characterization in a defined research area in northwestern Taiwan, the Miaoli Tableland. A detailed chronology of the sediment sequence is not in the scope of this morphological study.

2 Regional setting

2.1 Tectonic background and erosion rates of the Taiwanese mountain ranges and their foreland

The orogeny of the Taiwanese mountain ranges is caused by the arc-continent collision at the convergence zone of the Eurasian plate and the Philippine Sea plate in the western Pacific (Fig. 1a), which has been active since the Plio-Pleistocene (Suppe, 1984; Angelier et al., 1986; Teng, 1990; Willemin and Knuepfer, 1994; Teng, 1992; Yu and Song, 2000). Today, the mountain ranges of central Taiwan reach an elevation of 3952 m a.s.l. and are composed of Tertiary sedimentary rocks and low-grade metamorphic rocks at the western limb. Their westernmost part, a 10–20 km wide frontal belt has been called the "Western Foothills" (WF) (Fig. 1a) (Ho, 1988; Pelletier and Stephan, 1986) and has a general height below 2500 m a.s.l. The western foreland of the mountain ranges is a Neogene basin (Yang et al., 2006). The basin depositions have been interpreted as a succession of Tertiary sedimentary rocks overlain by Quaternary sediments yielded from the mountain ranges (Fig. 1a) (Simoes and Avouac, 2006; Yu and Chou, 2001; Lin and Watts, 2002; Lin et al., 2003; Chen et al., 2001; Ho, 1994; Covey, 1986). However, their precise chronology is not available yet (Ota et al., 2006; Chang et al., 1998; Teng, 1996b; Lin, 1963; Ho, 1994). Parts of these Quaternary sediments have been uplifted to present altitudes with a maximum height of ca. 1000 m a.s.l. Due to the complexity of the tectonism, the long-term uplift rates of the WF and the Neogene basin are still unclear (Deffontaines et al., 1997; Shyu et al., 2005; Yang et al., 2016; Teng, 1996a; Ching et al., 2011).

The strong uplift of the island and the subtropical monsoon climate including frequent typhoon events induce erosion rates with an average of 3–6 mm a^{-1} (Dadson et al., 2003). The precipitation is mainly concentrated during the summer and autumn; on average about two to three typhoons strike Taiwan annually (average 1949–2019) (Central Weather Bureau, 2019). Typhoons often cause extreme precipitation events and floods.

2.2 Quaternary sea-level change in Southeast Asia

The post-Last Glacial Maximum (LGM) sea-level curve of the Taiwan Strait has been established by radiocarbon dating of marine sediments (Liu et al., 2008; Chen and Liu, 1996). However, a pre-LGM sea-level curve is not yet established. The combination with global and regional models that reach back further, especially from the Sunda Shelf (Hanebuth et al., 2011; Shackleton, 2000), shows that the sea level was much lower than today after the end of the Eemian sea-level high stand, with a minimum during the LGM (−120 to −140 m). As the depth of the Taiwan Strait west of the Miaoli Tableland is less than 60 m, it was dry land during most of the Late Pleistocene (Horng and Huh, 2011; Huh et al., 2011), and the palaeoflow directions of the northwestern Taiwanese rivers were north to northeast toward the Kuanyin Depression (Huh et al., 2011) (Fig. 1a). After the general Holocene sea-level rise, a short-term high stand during the Mid-Holocene reached +5 m (Liu et al., 2004; Chen and Liu, 1996).

2.3 The tablelands in Taiwan

The uplift, sea-level changes, and the subsequent erosional processes have dissected the foreland sediments. These sedimentary terraces are called "-Ding/-頂" in the local language, i.e. terraces (Chen et al., 2004; Tomita, 1954) or tablelands (Tsai et al., 2010, 2006; Lin, 1957; Teng, 1979; Teng et al., 2001; Shih and Yang, 1985; Lin and Chou, 1978) according to different concepts of the landform evolution, respectively.

Tablelands are mainly distributed in a ca. 5–20 km wide area along the western margin of the WF (Fig. 1a), as well as in mountain basins. In the past, the tableland surfaces were differentiated morphologically and sedimentologically by the following criteria: (1) the lithification degree of the sediments, (2) the driving force of current morphology (fluvial incision/tectonic displacement), (3) the weathering characteristics of the cover sediments (relatively old and intensively weathered substrate/relatively young alluvial deposits), and (4) the elevation of surfaces as a relative chronological index of different morphological stages (Lin, 1957; Tomita, 1953, 1951, 1954). The resulting categories of the tableland surfaces were named "Laterite Highlands" for the higher-elevated quasi-flat surfaces that are covered by reddish, highly weathered sediments; "Laterite Terraces" for the lower-elevated quasi-flat surfaces that are covered by brownish/reddish highly weathered sediments; and "Fluvial Terraces" for the modern fluvial terraces/plains in the immediate vicinity of fluvial paths (Lin, 1957).

In recent decades there have been more detailed studies on the origin and development of the tablelands, e.g. studies on tectonism at the Dadu Tableland and Pakua Tableland (Delcaillau, 2001; Shih and Yang, 1985), the soil development and relative chronology at the Dadu Tableland (Tsai et al., 2010) and Pakua Tableland (Tsai et al., 2006), and the morphology and sediment chronology of the Puli Tableland (Tseng et al., 2013). The depositional environments and biostratigraphy of the sedimentary sequence as well as the morphology corresponding to active tectonism were studied in the Linkou Tableland (Horng, 2014; Teng et al., 2001) as well as the relative and absolute chronology, erosion, and tectonism of smaller terraces in other regions (Chen et al., 2004; Ota et al., 2009, 2002, 2005; Chen et al., 2003). All these studies gave a frame for an understanding of the tableland formation; however, neither an overall morphological model nor a detailed chronology of the tableland development has been established so far.

In past publications the terms "laterite/lateritic" have been used according to the local context, which describes the reddish/brownish, fine-grained soils on the surfaces. However, the usage of this term has recently been challenged by soil

studies (Tsai et al., 2010). According to the latest review of the soil taxonomy in Taiwan, these so-called laterite cover sediments on the tablelands have been revised as "Ultisols" or "Oxisols" by their chemical composition, respectively (Chen et al., 2015). To avoid over-interpretation of soil development characteristics and because the pedological factors of the sediments are not the subjects of this study, the following geomorphological descriptive terms are used in this text: "Sedimentary Highlands" (SH) for Laterite Highlands, "Sedimentary Terraces" (ST) for Laterite Terraces, and "Alluvial and Coastal Plains" (AL) for Fluvial Terraces.

2.4 Study area: the Miaoli Tableland

The sedimentary complexes in the Miaoli region are called the Miaoli Tableland (Teng, 1979) or Miaoli Hills (Chang et al., 1998). We prefer the former term because the geological and morphological settings of the area are consistent with the other tablelands in northwestern Taiwan (Lin and Chou, 1978; Teng, 1979). The Miaoli Tableland is located on the northwestern coast of Taiwan between the Houlong River and the Daan River (120°38′10″ to 120°48′57″ E, 24°36′51″ to 24°21′32″ N). Both rivers have their source area in the mountain belt and therefore a different hydrological regime than the other rivers in the study area. The Miaoli Tableland covers an area of ca. 283 km^2. Its topographical surface is characterized by terraces with different elevation levels. The highest elevation is located at the southernmost part at about 614 m a.s.l. This point is called "Huoyanshan/火炎山", also known as "Fire Mountain" (Fig. 1b). A narrow coastal plain forms a 30 km long stretch between the Wumei (Xihu) River and Yuanli River (Fig. 1b). It is composed of alluvial sediments that are carried by the longshore current (Jan et al., 2002; Wang et al., 2003); according to climate statistics from 2003 to 2020, the tidal difference in the shore area of Miaoli is 4–6 m (Central Weather Bureau, 2020).

The study area is mainly drained by the Tungxiao River and the Wumei (Xihu) River as well as other small local catchments (Fig. 1b). However, many of the fluvial paths in the area are artificially constrained by levees for defending from flooding. For example, the flooding which affected the Miaoli region on 7 August 1959 ("八七水災") was the most severe flooding in the 20th century in Taiwan (The Taiwan Provincial Weather Institution, 1959; Central Weather Bureau, 2019).

The geological maps and the studies of tectonic features exhibit one inferred syncline, two inferred anticlines with low dip angles, and four inferred thrust faults with steep dip angles in the study area (Fig. 1b). These features are almost parallel aligned, striking mainly northeast to southwest (Chang, 1990, 1994; Ho, 1994; Yu et al., 2013; Lin and Watts, 2002; Yu and Chou, 2001; Yang et al., 2016). The coastal area is affected by the tentatively called "frontal movement", which is assumed to be the youngest thrust movement in the Miaoli area (Shyu et al., 2005). Two active thrust faults have been identified at the eastern margin of the Miaoli Tableland (Ota et al., 2006), and an inferred thrust fault at the western fringe of the highlands has been proposed by Chang et al. (1998) (Fig. 1b). There are no direct studies on Quaternary uplift rates in the Miaoli area. Results from the southerly Pakua Tableland, based on radiocarbon dating of different heights of the terrace surfaces, show that it can be assumed to be around 1 mm a^{-1} (Ota et al., 2002, 2006).

The general formation of the Miaoli Tableland has been explained by two hypotheses. Chang et al. (1998) assumed that the present Sedimentary Highlands and the southwest of the Sedimentary Terraces area (the Pingding terrace, Fig. 1b) represent jointed alluvial fans. The gravels and cobbles, which build up the fans, were yielded from the Houlong, Wumei (Xihu), and Daan (palaeo-)rivers. The rest of the area (the Tungxiao River catchment) was interpreted as a palaeobay, which was subsequently filled with sediments (Appendix A). Following the traditional classification of Lin (1957), Chang et al. (1998) assumed that differentiated uplift and erosion during the late Quaternary have dissected the palaeotopography into terraces. They subdivided the surfaces of the Miaoli Tableland into the three surface elevation levels as Laterite Highlands, Laterite Terraces, and Fluvial Terraces (see Sect. 2.2).

In contrast, Ota et al. (2006) focused on differentiated tectonism in the Miaoli region. They assumed that folding along the Tungxiao Anticline (Fig. 1b) caused uplift in the present ST area. This induced the erosion of the overlying sediments, resulting in a topographic inversion along the anticline. The thrust of the Tongluo Fault (Fig. 1b) caused the uplift of the southern SH (tentatively named the "Sanyi Tableland"). This resulted in the separation of the ST and SH along a distinct topographic escarpment, which subsequently was rapidly eroded eastward causing the beheading of the valleys in the southern SH. Colluvial depositions of gravels and cobbles on the western slope foot of the escarpment exhibit the ongoing erosion (Chen, 1983).

The southeastern SH (former Laterite Highlands) is the most detailed studied part of the Miaoli Tableland. Ota et al. (2006) mapped massive, deeply dissected, and tectonically deformed fluvial terraces here. The strata are inclined $> 30°$ to the east in the Fire Mountain area (Chang, 1994). The inclination is assumed to be affected by the westward thrust of the Sanyi Fault (Yang et al., 2007) (Fig. 1b).

2.5 Former stratigraphical interpretations of the Miaoli Tableland

The stratigraphical interpretations of the sedimentary layers in the study area were proposed in the 1930s and redefined in the latter half of the 20th century. The sedimentary layers in the study area were described in different terms as follows.

2.5.1 Toukoshan Formation (Tk Formation)

The Tk Formation is the common term for the Pliocene–Quaternary strata that are exposed along the mountain front of the WF in northern and central Taiwan (Chang, 1990, 1994; Ho, 1994; Lee, 2000; Chen et al., 2001; Chang, 1953). However, information on the dimension and composition of the Tk Formation vary in the available publications. The composition is described as fine-grained sediments in the lower and coarse-grained fluvial sediments in the uppermost sections with a total thickness up to more than 1000 m in central Taiwan (Chang, 1948, 1955; Torii, 1935; Chen et al., 2001). The well-rounded shape of the fluvial gravels and cobbles shows that they might be reworked and transported over certain distances (Teng, 1996b). Some authors described the lower units as already consolidated (Chang, 1955; Ho, 1988; Chang, 1990). Biostratigraphical studies on planktonic foraminifera indicated that the deposition of the Tk Formation started after the end of Olduvai event (Huang, 1984), and a time span of 1.24–0.46 Ma was given by the comparison between the abundance of species and the biozones (Lee et al., 2002).

2.5.2 Tûsyô/Tungxiao/Lungkang Formation (Ts/Lk Formation)

Beside the broadly used term Tk Formation, an older definition of the sediment strata specifically in the Miaoli Tableland is called the Tûsyô Formation (as Ts Formation, according to pronunciations of Japanese of the local name "*通霄*"). It was proposed by Makiyama (1934, 1937) and renamed in Chinese as the Tungxiao Formation by Chang (1948) to describe the loose, poorly cemented sedimentary layers in the Miaoli Tableland with a sequence from bottom to top of intercalated marine sediments, tidal–coastal layers, gravel and cobble beds, and a surface layer with ocher-coloured soils. In 1963, Lin proposed the term Lungkang Formation (as Lk Formation) for the uppermost 10–15 m of the same succession in the coastal area of the Miaoli Tableland. The only difference between these two definitions is that the cover layer of the Lungkang Formation was interpreted as dune sand (Lin, 1963). The absolute chronology of these strata is uncertain. Makiyama (1934) assumed a late Tertiary deposition according to the composition of fossils by the palaeontological concept at that time. Radiocarbon dating on molluscs gave an early Holocene time span (Lin, 1969). The Ts/Lk Formation has been rarely mentioned by other authors after the 1960s.

2.5.3 "Alluvium Deposits", "Terrace Deposits", and "Lateritic Terrace Deposits"

These are different terms for the description of non-cemented deposits on various geographical surfaces (i.e. tablelands, valley floors, flood plains, coastal plains, and estuaries) in the geological maps of the study area (Ota et al., 2006; Chang et al., 1998; Chang, 1990, 1994; Ho, 1994; Chen et al., 2004). They are composed of gravel, aeolian sands, and a mixture of dusty fine sediments. No direct dating has been proceeded yet. A late Quaternary age was assumed based on the loose, poorly consolidated consistency of the deposits. The thickness of them varies depending to the palaeotopography; it reaches a maximum of about 20 m (Chang, 1990; Ho, 1994).

3 Material and methods

3.1 Terrain analyses

Systematic terrain analyses were undertaken by the combination and integration of 3D and 2D datasets: (1) open-access digital elevation models from the Ministry of the Interior of Taiwan (resolution 20 m) and the Shuttle Radar Topography Mission (SRTM, resolution 1 arcsec, ca. 80 m) (Satellite Survey Center, 2018; NASA JPL, 2013), (2) aerial photos and satellite imagery from the open-access Web Map Tile Service in a geographical information system (GIS) (Center for GIS RCHSS Academia Sinica, 2017; National Land Surveying and Mapping Center, 2016), (3) published topographic maps at a 1 : 25 000 scale accessible online (National Land Surveying and Mapping Center, 2016), and (4) geological maps of Taiwan (1 : 50 000) accessible online (Central Geological Survey, 2017).

For the identification and classification of different topographical landforms, we merged the information of absolute and relative elevation with the terrain steepness by applying automatic functions of the GIS software and manual mapping. The aim is to distinguish between the present fluvial paths, tableland surfaces, modern fluvial plains, and coastal plains as well as the slopes in between (Fig. 2).

Four terrain categories were defined:

- The category "fluvial paths" was derived from a calculation using the "Arc Hydro Tools" function in the GIS programme compared with the topographic maps and the aerial photos. The fluvial paths were mapped as line features, whilst other categories were mapped as surface features (polygons).

- The category "tableland" was defined as a quasi-flat surface with the following criteria: (1) the steepness is lower than 10°; (2) it is larger than 400 m^2 (1 pixel in the DEM); and (3) the flat surface is not in the direct vicinity of a flow path (Fig. 2). The steepness threshold was adapted from the study of Saito and Oguchi (2005), in which they proceeded the terrain analysis of 690 alluvial fans in Japan, Taiwan, and the Philippines. All fans show a terrain steepness lower than 7°; the majority of them have one less than 5°, including all 71 studied alluvial fans in this context in Taiwan (Saito and Oguchi, 2005). The edges of the tableland segments were determined by hand mapping. Comparing the direct raster to polygon conversion, it has concisely performed the noise reduction and the edge-smoothing pro-

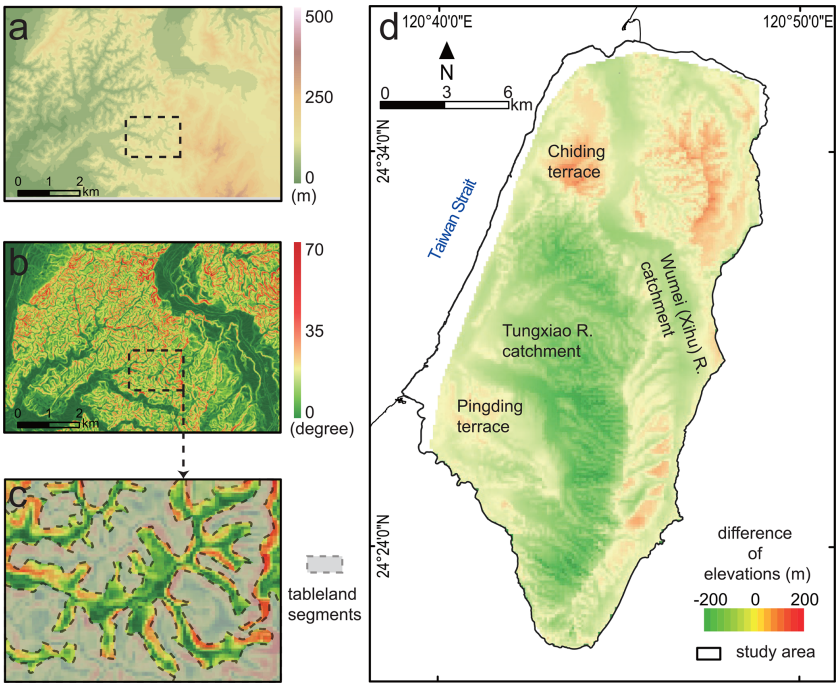

Figure 2. Mapping of the tableland segments. **(a)** The original digital elevation models (Satellite Survey Center, 2018). **(b)** Surface steepness was subsequently calculated by an ArcGIS function (slope). **(c)** An example of hand mapping of the tableland segments in GIS. The tableland segments were recognized by the gentle terrace surfaces. **(d)** Results of the calculation of relative surface elevations: negative values represent DEM elevations lower than the theoretical linear surface and vice versa. The spatial distribution of negative and positive values shows a clear separation at the divide of the Wumei (Xihu) River and the Tungxiao River catchments and at the southern margin of the Chiding terrace.

cedures. For a normalization of the general surface inclination of the Miaoli Tableland from the southeast to northwest, we calculated a theoretical linear-trend surface from the highest point of the terrain to the distal edge of the tableland surfaces, adapting the method of Volker et al. (2007), by using a triangulated irregular network (TIN) interpolation into a raster. Tableland areas above and below this theoretical linear-trend surface were defined as Sedimentary Highlands (SH) and Sedimentary Terraces (ST), respectively (Fig. 2d).

- Quasi-flat surfaces (less than 5°) in the immediate vicinity of the fluvial paths (e.g. valley floors) were defined as "modern fluvial plains". The "coastal plains" were defined as the plains which have a steepness less than 5° and an elevation lower than 30 m a.s.l. along the coast of the Taiwan Strait. The boundary of the plain was marked by the slope foot of the edge of the distal-tableland segments. The modern fluvial plains and the coastal plains were combined and defined as Alluvial and Coastal Plains (AL).

- The category "slopes" was defined for the rest of the surfaces which are steeper than 5°.

3.2 Field observations and sampling

The internal sedimentological composition of the tableland segments was studied to characterize and identify typical layer sequences throughout the study area; 51 field sites were chosen for a detailed description by the following criteria: the sites are (1) easily accessible and provide a good overview of the sedimentary layers, (2) evenly distributed across the study area, and (3) contain more than two visible sedimentary layers for a representative sampling and comparison with other outcrops.

The elevations of the sites were extracted from the DEMs and compared with a handhold GPS receiver in the field. The sedimentary layers in the outcrops were recorded by standard characteristics: shape of boundaries, thickness, sedimentary structures, texture, particle size, and visible fossil content (Miall, 2014; Vail et al., 1991). The sediment colour was only described in a general way to identify individual layers in the field. A specific determination of soil parameters as well as a detailed facies analysis of individual layers are not in the scope of this study. The sedimentary layers were identified in each field site independently, and then the records were compared to find identical layers and sequences throughout the study area. At 12 selected sites, 41 samples were taken for particle size analyses including 2 samples from modern beach (dune) sand for comparison.

3.3 Particle size measurements

The particle size analyses were conducted with a Beckman Coulter™ LS-13320 laser diffractometer at Section 3: Geochronology of the Leibniz Institute for Applied Geophysics, Hanover, Germany. This technique is well adapted for high-precision measurements of fine-grained particles smaller than 2 mm (Konert and Vandenberghe, 1997; Eshel et al., 2004; Beuselinck et al., 1998). None of the samples contained particles > 2 mm, even including the matrix of the gravel and cobble beds.

The sample preparations and measurements were proceeded as follows: for each sample, ca. 20–50 mg of the sediments was filled into the test tubes and treated with 1 % ammonium hydroxide (NH_4OH) solution, in order to disperse the aggregates of sediments for the subsequent particle size analyses. The test tubes were rotated for 24 h at 30 rpm to mix the solution and sediments. Organic matter was not removed. The particle size was measured five times for each sample to reduce the random error. The results were accepted when the value of polarization intensity differential scattering (> 80 %) and obscuration (< 10 %) passed both criteria. The statistical index of the coefficient of variance mean (< 5 %) and coefficient of variance standard variation (< 5 %) were chosen to evaluate the reproducibility of the results (Konert and Vandenberghe, 1997). The particle size fractions and the texture classifications (Jahn et al., 2006) were correlated for the characterization of sedimentary records.

4 Results

4.1 Terrain analyses – topography of the Miaoli Tableland

The topographical analyses reveal the proportion of different morphological categories in the study area: the tablelands (SH + ST) represent 24.2 % (ca. 68.7 km^2); the slopes and gullies represent 44.8 % (ca. 127.2 km^2); the fluvial plains represent 24.2 % (ca. 68.9 km^2); and coastal plains represent 6.6 % (ca. 18.7 km^2) (Fig. 3).

The tableland surfaces are unevenly spread throughout the study area. Their sizes vary from only a few hundred square metres to several square kilometres. The larger tableland segments with widths ranging from ca. 100–1500 m, such as Pingding (ca. 7.0 km^2), Chiding (ca. 4.3 km^2), and other parts (from 2.0 to 0.5 km^2) represent ca. 14 % of the total terrain. However, the high-resolution mapping revealed that the overall spatial pattern of the tableland surface is made up of numerous smaller segments, which are only ca. 40–200 m wide (Fig. 3). They generally represent the water divides between the fluvial paths and are broadly distributed in the study area. Their distribution and shape depend also on different fluvial drainage patterns in the study area.

Figure 3. Results of the terrain analyses and the classification of tableland segments. The Sedimentary Highlands (SH) represent the fluvial terraces, located in the southeastern (SH-I) and northern part (SH-II) divided by the Wumei (Xihu) River. The Sedimentary Terraces (ST) are mainly located in the Tungxiao River catchment. The Alluvial and Coastal Plains (AL) represent the flat surfaces beside the fluvial channels. Detailed mapping of drainage patterns and the elevation profiles of the fluvial valleys is presented in Fig. 4.

The differentiation between the SH and ST can be clearly inferred from the relative height between the true elevations and the theoretical linear-trend surface (Fig. 2d). Furthermore, both show different directions of their inclination in general. The SH is composed of tablelands with ca. 2° northwest-inclining surfaces, while the ST tableland surfaces incline ca. 1° to the west (Fig. 3).

The topographical divide between the ST and the SH is represented by a continuous, west-facing escarpment bending from the southeast to the northwest. The steepness of the slope is about 30° and more. Its relative height is ca. 130–200 m in the south, decreasing northwestward to about 30 m.

4.1.1 The Sedimentary Highlands (SH)

The Sedimentary Highlands (SH) are located in the east and the north of the study area. They were divided into two subgroups by their surface elevation and their location with respect to the Wumei (Xihu) River. The area south of the Wumei (Xihu) River with elevations of about 250 to 614 m a.s.l. is named SH-I. These tableland surfaces are dissected to a minor degree and incline quasi-continuously northward to the left bank of the Wumei (Xihu) River (Fig. 3). The fluvial paths incised in the SH-I segments flow to the northeast. They are tributaries of the Wumei (Xihu) River and show a parallel pattern. The tableland in the northern and the northwestern part of the study area with elevations between 30 and 250 m a.s.l. is classified as SH-II (Fig. 3). The tableland segments are separated by the Wumei (Xihu) River into a western and an eastern part. The western part has larger coherent tableland surfaces, i.e. the tableland segment in Chiding, which is here the topographical divide between the Wumei (Xihu) River and the Taiwan Strait. The eastern SH-II is well dissected, and the remaining tableland segments are the interfluves between the tributaries of the Wumei (Xihu) River, the Nanshi River, and the Houlong River (Fig. 3). The fluvial paths between the SH-II segments are mainly below 150 m a.s.l. and have formed dendritic drainage patterns. All these streams flow in a western or northwestern direction to join the Wumei (Xihu) River and Houlong River or directly to the coast, respectively.

4.1.2 The Sedimentary Terraces (ST)

The Sedimentary Terraces (ST) are located to the west of the SH-I. They are distributed over the whole Tungxiao River catchment and extend further south to other smaller catchments. The majority of ST is lower than 250 m (the highest point is 445 m a.s.l., located at the boundary to the SH-I) and dropping to ca. 30 m at the distal edge close to the coast (Fig. 3 and Appendix A). The larger tableland segments (i.e. Pingding) are located south of the main stream of the Tungxiao River. The smaller tableland segments make up the bulk of the ST surfaces and can be connected tentatively by a quasi-flat inferred surface through the whole ST area (Fig. 3). Their topographic height is ca. 30 m in the east and decreases westward to ca. 5 m at the distal-tableland segments.

The drainage patterns in the ST are differentiated by the elevation. Streams above 150 m a.s.l. form a parallel drainage pattern similar to the SH-I (Fig. 3). Most of them begin near the topographic escarpment (i.e. western slope of the SH-I), and their flow path gradients vary from 1.0 to 14.0° (Fig. 3). The streams below 150 m a.s.l. in the central and western part of the ST have formed dendritic drainage patterns. The fluvial pattern in the SH-II shows also a dendritic system.

4.1.3 Slopes

The gradient of the slopes ranges from 10 to 66° with a majority of 10 to 26°. The spatial distribution of the gradients clearly shows a pattern in different scales. At an overall scale, the slopes in the north and west are gentler than the slops in the south and east, while the differences between individual slopes are not so distinct. In the areas of the dendritic drainage patterns, the vertical shape of the slopes tends to be concave; i.e. the upper part of the slope is steeper than its foot. Reversely, in the areas of the parallel drainage patterns, the vertical shape of the slope is more convex (Fig. 4). Thus, the sections of the upper valleys above 150 m are typically V-shaped.

4.1.4 The Alluvial and Coastal Plains (AL)

The Alluvial and Coastal Plains (AL) reach elevations up to 150 m a.s.l. and represent the wide valley floors and the coastal area (Fig. 3). The main streams' flow paths have gradients from 0.1 to 0.2°, whereas the tributaries' flow paths are steeper (up to 8.0°). The majority of them are braided rivers, except the meandering Nanshi River, a tributary to the Houlong River (Fig. 3). The valley width is not consistent. It is up to kilometres in the main streams and ca. 20–100 m in most of the tributaries. Therefore, the AL represents the active fluvial plains as well as the terraces adjacent to the fluvial paths with one or two levels. The relative height of these terraces is < 10 m. Their sizes are constrained by their location and the stream order. The larger ones ($> 1\,km^2$) in the vicinity of main streams are up to 2100 m wide; the smaller ones ($< 1\,km^2$) in the tributaries are ca. 20–40 m wide (Fig. 3). The AL occurs only in those areas of the SH-II and ST with a dendritic drainage pattern. The valleys are ca. 150–1300 m wide and ca. 20–50 m deep and show relatively narrow flow paths (< 10 m mostly) (Figs. 3 and 4 and Appendix A). In combination with the steep slopes, valley cross sections show a quasi-rectangular transverse profile for which we introduce the term "box-shaped valley".

The coastal plain has a consistent width of around 500–1000 m, but it widens up to 1500 m in the area of the estuaries. The topographic boundary between the coastal plain and distal-tableland segments can be clearly identified by the slope foot of the tableland segments (Fig. 3).

4.2 Sediment descriptions

The 51 studied outcrops in the Miaoli Tableland are located at the edges of the tableland segments (Fig. 5, Table 1) and provide therefore a vertical insight into their internal composition.

Their height ranges from about 3 to 50 m, and they are characterized by up to six relevant unconsolidated sediment layers (Figs. 5 and 6). However, only two of the outcrops show all layers of the succession (i.e. 001_HLPT and 010_EFB). Only a limited number of layers is exposed in

Table 1. List of studied outcrops.

No.	Name	Latitude	Longitude	Location	Height (m)	Elevation (m a.s.l.)
1	HLPT (Hou-Long Petroleum)	24°35′45.30″ N	120°48′24.01″ E	SH-II	49	37
2	BTL (Ban-Tian-Liao)	24°35′47.02″ N	120°43′38.77″ E	SH-II	6	73
3	CSW (Chiuan-Shuei-Wo)	24°35′6.78″ N	120°48′28.61″ E	SH-II	7	97
5	RSK (Rong-Shu-Keng)	24°34′37.68″ N	120°44′23.69″ E	SH-II	4	74
6	NBK (Nan-Bei-Keng)	24°34′21.97″ N	120°44′6.16″ E	SH-II	8	105
7	NCT (Nan-Ching Temple)	24°34′19.24″ N	120°43′32.91″ E	SH-II	3	71
8	MYK (Ma-Yuan-Keng)	24°34′2.42″ N	120°46′48.54″ E	SH-II	6	165
9	LG (Long-Gang)	24°34′1.12″ N	120°48′21.08″ E	SH-II	4	116
10	EFB (Er-Fu Bridge)	24°33′50.55″ N	120°44′48.17″ E	SH-II	11	28
11	FTK (Fu-Tou-Keng)	24°33′37.89″ N	120°44′21.63″ E	SH-II	10	107
12	ZW (Zhang-Wo)	24°32′50.93″ N	120°46′36.74″ E	SH-II	7	68
13	TKD (Tu-Kan-Ding)	24°32′23.29″ N	120°42′27.86″ E	ST	3	148
15	XP (Xin-Pu)	24°32′8.56″ N	120°41′41.95″ E	ST	3	10
17	BW (Bei-Wo)	24°31′12.20″ N	120°43′3.51″ E	ST	6	26
18	DBD (Da-Bi-Dou)	24°30′54.09″ N	120°43′14.00″ E	ST	8	46
20	GCW (Gu-Cuo-Wo)	24°29′48.64″ N	120°44′55.34″ E	ST	5	94
22	ZG (Zhu-Gang)	24°28′55.02″ N	120°42′8.09″ E	ST	20	21
23	XNPW (Xiao-Nan Power Substation)	24°28′17.69″ N	120°40′12.99″ E	ST	2	29
24	YZS (Yuan-Zih-Shan)	24°27′45.38″ N	120°43′15.15″ E	ST	6	67
25	JJC (Jin-Ji Company)	24°27′31.52″ N	120°39′48.64″ E	ST	7	16
26	SLK (Shiau-Lan-Keng)	24°25′45.22″ N	120°44′37.25″ E	ST	7	227
27	TZK (Tian-Zih-Keng)	24°25′58.22″ N	120°41′24.60″ E	ST	5	47
28	HDK (Hu-Dong-Kou)	24°34′49.79″ N	120°45′48.85″ E	SH-II	4	50
29	GJW (Gong-Jiao-Wan)	24°31′14.41″ N	120°47′29.54″ E	SH-II	7	179
30	TYGC (Tiao-Yan-Gu-Chi)	24°26′51.29″ N	120°45′13.33″ E	SH-I	5	335
31	XNPWH (Xiao-Nan Power Substation Heights)	24°28′15.05″ N	120°40′17.79″ E	ST	2	38
32	THST (Dong-He Steelworks)	24°34′13.42″ N	120°44′27.13″ E	SH-II	3	75
33	SZZ (San-Zuo-Wu)	24°22′14.62″ N	120°42′41.03″ E	ST	11	177
34	ZNQ (Zhong-Nan Quarry)	24°30′19.62″ N	120°41′23.91″ E	ST	5	25
35	YCZ (Yu-Cuo-Zhuang)	24°23′59.15″ N	120°42′17.68″ E	ST	10	118
36	KNS (Keng-Nei South)	24°35′12.39″ N	120°46′34.24″ E	SH-II	6	50
37	PD (Ping-Ding)	24°28′2.00″ N	120°41′0.36″ E	ST	7	64
38	JJW (Jie-Jih-Wo)	24°29′6.06″ N	120°43′44.16″ E	ST	5	70
39	JSS (Jin-Shan South)	24°24′58.39″ N	120°41′43.93″ E	ST	27	117
40	RGK (Lei-Gong-Keng)	24°32′32.61″ N	120°46′53.79″ E	SH-II	7	96
41	CHL (Chung-He-Li)	24°35′38.90″ N	120°44′16.56″ E	SH-II	10	55
42	GGF (Guo-Gang Fossils)	24°36′17.61″ N	120°43′49.20″ E	SH-II	4	18
43	SLP (Shuei-Liou-Po)	24°25′59.15″ N	120°41′42.66″ E	ST	10	60
44	NZ (Nan-Zhuang)	24°28′28.28″ N	120°43′21.62″ E	ST	7	63
45	SFK (Shuang-Fong-Kou)	24°28′43.12″ N	120°47′50.39″ E	SH-II	6	192
46	SFB (Shuang-Fu Bridge)	24°30′50.62″ N	120°42′48.73″ E	ST	10	28
47	XBW (Xia-Bei-Wo)	24°31′27.81″ N	120°44′4.72″ E	ST	10	55
48	CTC (Chih-Tu-Ci)	24°35′3.58″ N	120°43′36.15″ E	SH-II	4	69
49	HBK (Hong-Beng-Kan)	24°25′49.87″ N	120°42′33.61″ E	ST	4	121
50	LD (Long-Dong)	24°32′38.91″ N	120°46′29.13″ E	SH-II	2.5	79
51	LK (Long-Kang)	24°36′37.61″ N	120°44′52.69″ E	SH-II	9	3
52	NWII (Nan-Wo II)	24°30′5.68″ N	120°43′53.50″ E	ST	7	57
53	CLK (Che-Lun-Keng)	24°25′51.17”N	120°43′32.89”E	ST	2	157
54	JW (Jiang-Wo)	24°33′3.55″ N	120°45′54.91”E	SH-II	10	34
56	IFF (Yi-Fang Farm)	24°32′29.53″ N	120°46′52.54″ E	SH-II	6	86
57	CTK (Chang-Tan-Keng)	24°26′12.68″ N	120°46′19.75″ E	SH-I	30	301

Note: 57 outcrops were documented initially, but 6 of them were excluded because of visible disturbances.

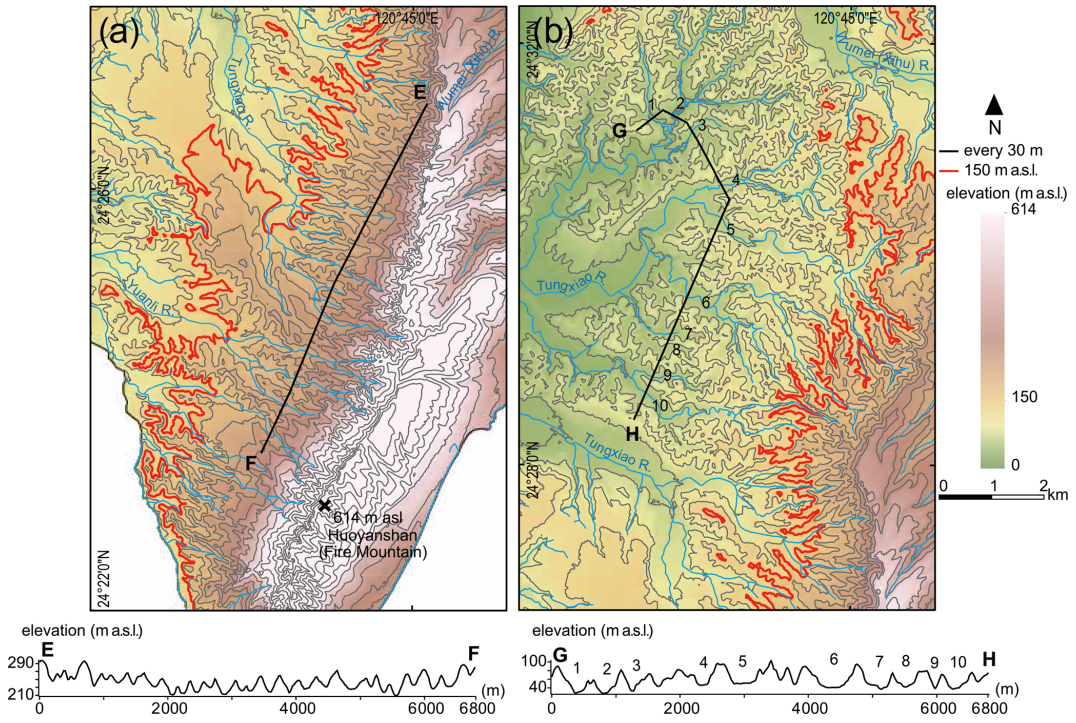

Figure 4. Detail maps of different fluvial drainage patterns in the Sedimentary Terraces (ST) with the respective elevation profiles of the valley cross sections. **(a)** Parallel patterns near the west-facing topographic escarpment between the SH-I (southeast) and ST (northwest) with valley bottoms mostly higher than 150 m a.s.l. Profile E–F shows the typical V-shaped valley cross sections. **(b)** Dendritic patterns in the northern ST area, especially with valley bottoms lower than 150 m a.s.l. Profile G–H shows wider and mainly box-shaped valley cross sections.

the rest of the outcrops – in general the upper part of the sequence. The layers were named according to their grain size composition applying the classification of the FAO (Food and Agriculture Organization of the United Nations; Jahn et al., 2006). They are from bottom to top (1) greyish loam (L), (2) loamy sand (LS), (3) alternations between greyish and yellowish silt loam (SiC), (4) sandy loam (SL), (5) gravel and cobble bed (CSB), and (6) silty loamy cover layer (SiL). The results of their respective grain size properties are listed in Table 2 and summarized in Fig. 7.

4.2.1 Greyish loam layer (L)

This layer is exposed only in three outcrops (01_HLPT, 10_EFB, and 025_JJC; Figs. 5 and 6 and Appendix C). They are located in the north of the SH-II and in the west of the ST. The upper 7 m of the layer are visible, but its total thickness is unclear, as the lower boundary is not exposed (Fig. 6). The upper boundary of this layer is even, continuous, and very distinct. Its internal structure is simple and massive; i.e. no bedding or laminae are visible. The sediment is poorly consolidated. However, it is quite sticky and difficult to excavate with hand tools. The grain size proportions range from 39 % to 52 % sand, 37 % to 48 % silt, and 11 % to 15 % clay, based on three samples (Fig. 7). This layer contains abundant mollusc detritus, which is poorly oriented and mixed with the sediments without layering for identifying the palaeoflow direction.

4.2.2 Loamy sand layer (LS)

This layer is exposed in outcrops of the tablelands ST and SH-II ($n = 16$) (Fig. 6 and Appendix C). It is ca. 5–20 m thick. The internal structure of this layer is simple and massive. At some outcrops, thin layers (less than 1 cm) with iron coating are recorded at the upper 50 cm. The sediment is very poorly consolidated and easily to scratch by hand tools. The dominating grain size in the five samples is sand (62 %–88 %). Two of them show a slightly higher content of silt. The clay content is less than 10 % in all samples. The texture is in the range of sand to sandy loam (Fig. 7). This layer's biological content is too low to be distinguished macroscopically.

4.2.3 Alternation of greyish silt loam and yellowish silt loam layers (SiC)

These sediments are exposed in outcrops ($n = 27$; see Fig. 6 and Appendix C) at the tablelands of the ST and SH-II. Their thickness is ca. 10–15 m. The layer is also visible on the tidal flat in outcrop 051_LK during the neap tide. The internal

Table 2. Results of grain size analyses.

Sample ID	Layer	Sand (%)	Silt (%)	Clay (%)	Sediment texture (Jahn et al., 2006)
LK 0-4 sand dune 0-1	Modern beach sand	97.0	1.8	1.2	Sand
LK 0-4 sand dune 0-2	Modern beach sand	97.0	1.9	1.2	Sand
HLPT 0-7	SiL	45.3	43.1	11.6	Loam
NCT0-3	SiL	51.0	37.9	11.1	Loam
XNPW0-2	SiL	46.1	42.7	11.1	Loam
HDK0-4	SiL	34.8	50.2	14.9	Silt loam
TYGC-2	SiL	22.6	57.1	20.3	Silt loam
XP-1	SiL	44.2	39.7	16.2	Loam
XNPWH-2	SiL	43.0	42.2	14.7	Loam
TKD-3	SiL	50.9	36.7	12.4	Loam
JJC-2	SiL	38.8	44.0	17.1	Loam
HLPT 0-6	CSB	37.7	42.3	20.0	Loam
TKD-2	CSB	48.7	34.9	16.4	Loam
HLPT 0-5	SL-b	39.4	41.9	18.7	Loam
NCT0-2	SL-b	44.7	40.0	15.3	Loam
XNPW0-1	SL-b	25.3	53.6	21.1	Silt loam
DBD0-1	SL-b	50.3	42.4	7.3	Loam
XNPWH-1	SL-b	44.3	40.1	15.6	Loam
GJW-2	SL-b	32.8	47.3	19.9	Loam
TKD-1	SL-b	41.6	43.5	14.9	Loam
JJC-1	SL-b	42.3	40.9	16.9	Loam
NCT0-1	SL-y	60.4	29.8	9.8	Sandy loam
HDK0-1	SL-y	79.0	15.9	5.1	Loamy sand
HDK0-2	SL-y	71.3	21.4	7.3	Sandy loam
HDK0-3	SL-y	66.3	23.9	9.8	Sandy loam
LK 0-1	SL-y	89.3	7.7	3.0	Sand
LK 0-2	SL-y	89.9	7.2	2.9	Sand
LK 0-3	SL-y	73.0	19.8	7.2	Sandy loam
THST-1	SL-y	84.0	11.2	4.7	Loamy sand
THST-2	SL-y	56.3	32.4	11.4	Sandy loam
TYGC-1	SL-y	70.8	21.8	7.5	Sandy loam
LK 0-5 yellowish loam	SiC	22.9	68.0	9.2	Silt loam
LK 0-5 greyish silt loam	SiC	8.3	79.7	12.0	Silt loam/silt
HLPT 0-2 001	LS	86.7	10.3	3.0	Sand
HLPT 0-3 001	LS	70.4	25.0	4.7	Sandy loam
HLPT 0-4 upper	LS	85.6	11.4	2.9	Sand
LK 0-6	LS	88.2	8.4	3.4	Sand
LK 0-7	LS	62.4	31.6	6.0	Sandy loam
HLPT 0-1 middle	L	40.5	44.3	15.2	Loam
JJC-A-1	L	39.2	48.0	12.8	Loam
JJC-A-2	L	51.6	37.7	10.7	Loam

structure shows thin beds of (I) the yellowish sandy sediments and (II) greyish clayey and silty sediments (10–100 layers with ca. 5–10 cm thickness of each layer) (Fig. 6). Iron precipitation can be distinguished on the contacts between these thin beds. The sediments are generally poorly consolidated; the greyish sediments are stickier than the yellowish sediments. Silt is the dominating grain size in both sublayers (68 %–80 %), of which the yellowish one has a certain sand content (23 %, Fig. 7). No molluscs or other biological remains are distinguishable in this layer.

4.2.4 Sandy loam layer (SL)

This ca. 10–30 m thick layer is exposed in outcrops across the entire study area ($n = 43$) (Fig. 6 and Appendix C). The upper contact to the overlying gravel and cobble bed (CSB) is continuous and very distinct. However, the contact is difficult to distinguish when the CSB is missing, and this layer is overlain directly by the silty loamy cover layer (SiL) (Fig. 6 and Appendix A). The sedimentary texture of this layer shows significant vertical variations among the outcrops and is therefore subdivided into three categories. (I) The light

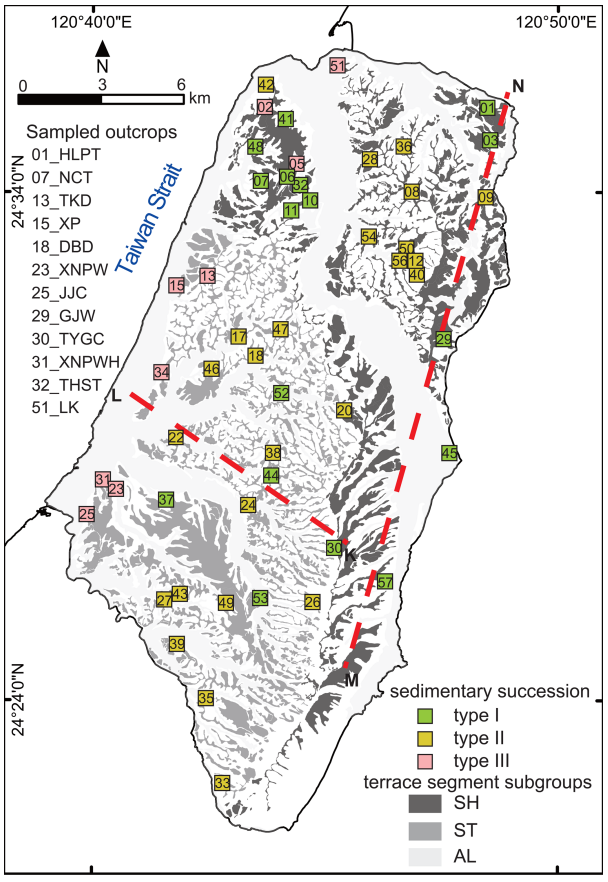

Figure 5. Location of the 51 studied outcrops (see Table 1); 26 outcrops are located in the SH, and 25 outcrops are in the ST. The 12 sampled outcrops for the grain size analyses are listed (see Table 2 for results). For profiles K–L and M–N and sedimentary subtype description, see Fig. 8.

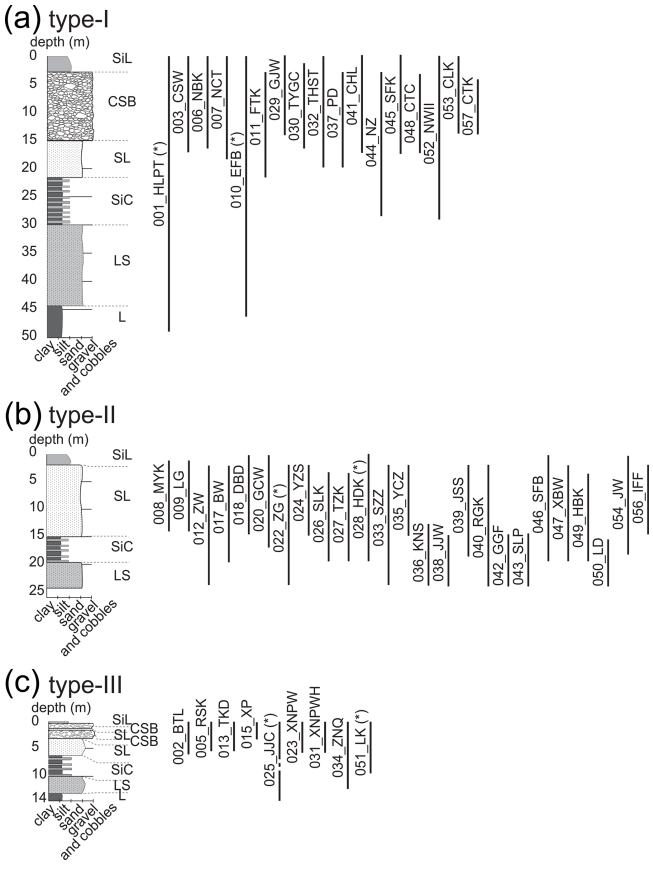

Figure 6. Schematic profiles of different sedimentary successions in the SH-II and ST with the respective outcrop numbers. **(a)** Type I: complete succession, located mainly in the larger tableland segments. **(b)** Type II: incomplete succession with the missing gravel and cobble bed ("remnants"), located mainly in the smaller tableland segments. **(c)** Type III: the succession with one or more thin gravel and cobble bed(s), located in the distal-tableland segments near the coast. Sediment layers are named after the FAO classification (Jahn et al., 2006): L – greyish loam, LS – loamy sand, SiC – alternations of greyish silt loam and yellowish silt loam, SL – sandy loam, CSB – coarse sand with stones and boulders (gravels and cobbles), and SiL – silty loam (cover layer). (*) Vertical lines indicate the relative depth of the outcrops with the respective sediment layers, which are visible in the field. The metrical depth scales are taken from the representative outcrops for each succession type.

greyish sandy material is in the lower metres (SL-g, not sampled). (II) The yellowish sandy material is in the middle part (ca. 5–10 m), which contains more than 50 % and – in two samples – nearly 90 % sand (SL-y) (Fig. 7). The upper ca. 1 m consists of brownish sandy loamy substrate (SL-b) with more than 40 % silt. The sediments in all three subtypes are very poorly consolidated; only the brownish sediments are stickier. The overall internal structure of SL-g and SL-b is massive. In the SL-y, iron coating in thin beds is visible. Debris of molluscs can be found in this layer; especially outcrop 035_YZS contains abundant detritus of molluscs.

4.2.5 The gravel and cobble bed (CSB)

Gravel and cobble beds are widely distributed in the Miaoli Tableland and exposed in 26 outcrops (Figs. 6 and 7 and Appendix C). Their thickness is varying according to the location: ca. 5–20 m in the SH-II, < 10 m in the ST, and < 2 m in the distal edge of the tableland. The sedimentary structure of the layer is mostly clast-supported but is matrix-supported in some outcrops at the distal edge of the tableland. Therefore the layer is classified as "coarse sand, with stones and boulders" (CSB) according to Jahn et al. (2006). In the clast-supported outcrops, the gravels are horizontally aligned with the long axes. The imbrication is poor; therefore, a precise analysis of flow directions is not possible. The gravels and cobbles consist of quartzite. Their sizes range from ca. 10 to 40 cm in the SH-II and from < 10 to ca. 30 cm in the ST. The gravels are well-rounded; their sphericity is moderate to platy.

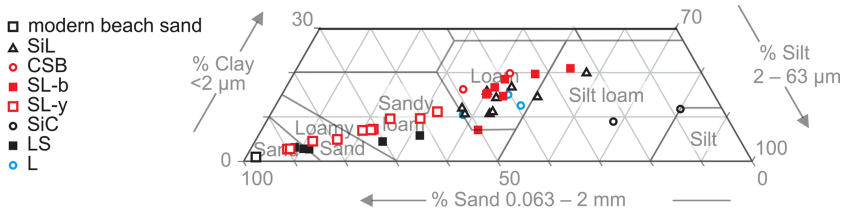

Figure 7. Grain size compositions presented in a combined ternary diagram; the samples were grouped for the respective sediment layers. The sandy loam layer (SL) is subdivided into the lower SL-y and the upper SL-b. The clay content in the samples is relatively constant, while sand and silt change significantly. Sediment nomenclature after Jahn et al. (2006). For detailed grain size distribution curves, see Appendix B.

The matrix material in the two samples taken from outcrops in the distal-tableland area is loamy; it consists of ca. 80 % sand and silt. The CSB in the distal tableland contains biological remains such as roots and wood debris.

The situation in the SH-I is different. Here the gravel and cobble bed is more than 20 m thick, and its elevation above the sea level is higher than in the SH-II and the ST. Its lower boundary is rarely visible. In the southernmost part of the SH-I (i.e. Fire Mountain), the gravel and cobble layer is inclined (estimated to be ca. 30°) to the east, which is in accordance with the records from the geological maps. Unfortunately, they are accessible only in few locations. The two studied outcrops show well-rounded quartz gravels and cobbles from 10–40 cm with poor imbrication.

4.2.6 Silty loamy cover layer (SiL)

The dusty cover layer can be found across the entire study area ($n = 25$) with a thickness from tens of centimetres up to 1.5 m (Fig. 6 and Appendix C). Its lower boundary, especially to the CSB, is very distinct. Its internal structure is simple and massive. It consists of a yellowish to reddish mixture of sand (35 %–51 %) and silt (30 %–44 %); clay occurs at 12 %–20 %. Only two of the nine samples have a silt content higher than 50 % (Fig. 7). The sediment is very loose and contains abundant fresh roots of the modern vegetation.

4.3 Subtypes of the sedimentary succession

The described sedimentary succession is unevenly exposed in the study area. Most outcrops show only a limited number of the layers. However, layers in neighboured outcrops can be recognized and linked over most of the study area. Nevertheless, small variations in the sedimentary succession have been recognized. Three subtypes of the layer assemblage were observed (Figs. 5, 6, and 8 and Appendices A and C): (I) the complete succession, (II) the quasi-complete succession with a missing gravel and cobble layer, and (III) the presence of a thin gravel and cobble bed(s) on the surface (0–3 m).

Type I is widely distributed in larger tableland segments of the SH-II and the ST (Figs. 5 and 8). The outcrops comprise identical sedimentary successions, and the gravel bed (CSB) is getting thinner toward the coast. The complete succession is exposed with all layers only at two locations (001_HLPT and 010_EFB). However, also the smaller outcrops show an order of the layers, which is in accordance with the complete succession (Figs. 6 and 8).

The sedimentary succession in the SH-I is still unclear. The two studied outcrops contain a very thick gravel and cobble layer (> 20 m mainly). Subjacent sandy substrate is only exposed in outcrop 030_TYGC. Therefore, the sedimentary succession of the SH-I is named "quasi-type I", because the sedimentary succession below the gravel unit is virtually unknown (Fig. 8).

Type II is found at the smaller tableland segments of the ST and the SH-II (Figs. 5 and 8). The outcrops include all the fine-grained sedimentary layers, but the overlying gravel and cobble layer is missing. In most outcrops in the SH-II, a sequence of LS–SiC–SL–SiL is exposed (Figs. 6 and 8). In contrast, the outcrops in the ST show a relatively thick layer of SL (ca. 20 m or more), while the L, LS, and SiC layers are rarely exposed.

Type III occurs in the ST and the SH-II along the fringe of the distal-tableland segments and at the coast (Figs. 5 and 8) at elevations below 50 m a.s.l. It includes SL, SiC, SiL, and L at the lower part and one or two thin (< 2 m) gravel and cobble bed(s) intercalated with sandy (SL) layers on the upper part to the surface (Figs. 6 and 8). The gravel bed(s) is getting thinner coastward.

Beside the gravel and cobble beds in the tableland segments, gravels and cobbles occur in the AL as well. For example, abundant gravels and cobbles are deposited in most of the fluvial paths especially in tributaries of the Tungxiao River within areas with dendritic drainage patterns (Appendix A). According to the field observations, these gravels and cobbles are composed of quartzite, their shapes are round, but the components are poorly sorted.

5 Discussion

The general topography of the Miaoli Tableland inclines from the highland in the southeast towards the coast in the north and in the west. A clear spatial separation of three main areas can be distinguished: the Sedimentary Highlands in the southeastern part (SH-I) and in the northern part (SH-II) as

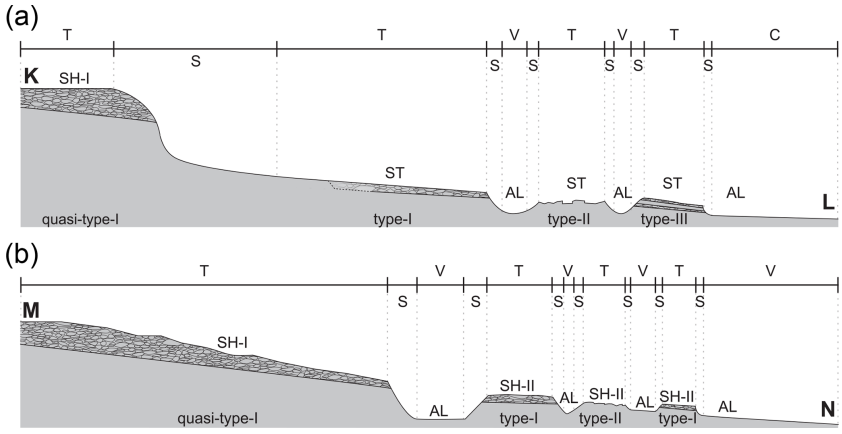

Figure 8. Schematic surface elevation profiles from **(a)** the highlands to the coastal plain through the SH-I and the ST (K–L) and **(b)** the highest point (i.e. Fire Mountain) to the Houlong River through the SH-I and the SH-II (M–N). The terrain categories and the corresponding subtypes of the sedimentary succession are marked (T: tableland segment, V: valley floor, C: coastal plain, and S: slope).

well as the Sedimentary Terraces (ST) in the western part. Especially the cliff-like topographic divide between the SH-I and the ST is a distinctive topographic landscape element in the Miaoli Tableland. This elevation-data-based topographical classification agrees in general with previous findings (Chang et al., 1998; Ota et al., 2006). However, the high resolution of the DEMs reveals that the topography of the tableland is much more disaggregated into larger and smaller segments than previously mapped. These segments cover most of the area of the Miaoli Tableland, and their surfaces can be tentatively connected or geometrically interpolated to an inferred palaeotopography in the respective areas (Figs. 2d and 3).

The internal sedimentary succession of the tableland segments is consistent in the SH-II and the ST areas but different in the SH-I. The individual strata of the SH-II and ST appear in the same order. The lower to middle part of the studied sedimentary sequence (L–LS–SiC–SL) represents an intertidal to supratidal deposition sequence, which has been reported by case studies in various locations globally (Goodbred and Saito, 2011; Dalrymple and Choi, 2007; Chen et al., 2014; Olariu et al., 2012; Buatois et al., 2012). This general tidal-dominant environment setting is consistent with the interpretation of the study of molluscs and foraminifera taken from this succession previously (Lee et al., 2002; Lin, 1969), although their stratigraphical context is not clear in detail. It is possibly due to sea-level changes (Shackleton, 2000) and long-term uplift of the Miaoli area (Ota et al., 2006; Yang et al., 2016). The distinct boundaries of each sedimentary layer may result from the interruption of sedimentation or the subsequent erosion, especially during the aforementioned regression periods (Davis, 2012).

Depending on the location, the studied sequence is topped by units of fluvial gravels and cobbles with different thickness. Previously, tablelands were identified by their flat surface and the occurrence of gravels and cobbles on their surface (Chang et al., 1998; Lin and Chou, 1978; Teng, 1979). We found that this is mainly the case for the larger and also some smaller segments, which represent sedimentation type I (Figs. 5 and 8 and Appendix A). On most of the small segments, the gravels and cobbles are missing (type II, Figs. 5 and 8 and Appendix A). However, the inferred palaeotopography implies a formerly continuously distributed gravel and cobble layer in the ST and the SH-II, where the smaller segments represent remnants, from which the gravels and cobbles were eroded. The fact that gravels and cobbles are also accumulated in the channels between segments with missing a gravel and cobble layer supports the idea that they were reworked from higher positions on the ST and the SH-II into the AL. This is new in comparison with Chang et al. (1998) and Ota et al. (2006), who did not assume a continuous gravel and cobble layer in the ST and SH-II area. In the distal segments near the coast, the gravels and cobbles tend to be smaller and occur in several thin layers (type III, Figs. 5 and 8 and Appendix A); thus we assume that the gravels and cobbles are reworked from the nearby sources (i.e. the proximal segments and remnants in the SH-II and ST).

The clast-supported structure and the moderate sorting of the fluvial deposits indicate that the deposition occurred rapidly, assumably during high-precipitation and discharge events. These characteristics are similar to the gravel and cobble beds in the other tablelands in northern Taiwan (Teng, 1996b). Although Chang et al. (1998) measured the cobble imbrication at several locations, we were not able to confirm their results due to the poor conservation of the sampling sites in recent decades. Moreover, the sphericity of the gravels and cobbles in our outcrops hinders the reconstruction of individual transport directions.

Regardless of the occurrence of gravels and cobbles, the whole area is covered by a layer of fine-grained material (SiL), which has been interpreted as the in situ lateritic soil formation before (Chang et al., 1998; Ho, 1988; Chang,

1955). However, the grain size data yielded a high content of fine silt rather than clay in this layer (Fig. 7). The fine silt is typical for aeolian transport (Pye and Zhou, 1989). Therefore, this study follows the assumption of a significant aeolian dust input (Chen et al., 2013; Tsai et al., 2008; Hebenstreit and Böse, 2015) besides the local weathering. Dust transport may also explain the silt enrichment in the upper part of the SL layer.

The whole sedimentary sequence in the SH-II and the ST is in agreement with the descriptions in early sedimentary studies of the Miaoli Tableland, where it has been named the Lungkang (Lk) Formation (Lin, 1963, 1969) or Tûsyô/Tungxiao (Ts) Formation (Chang, 1948; Makiyama, 1934, 1937). This study refers to those definitions because they are based on the descriptions of the uppermost 50–100 m of the succession directly in the study area, although the former studies tended to use the term Toukoshan (Tk) Formation (Chang, 1955), which includes however the whole Plio-Quaternary strata in western Taiwan (Chen et al., 2001; Ota et al., 2006; Lee et al., 2002; Huang, 1984; Tsai et al., 2006; Yang et al., 2016).

Early studies assumed that all fine-grained sediments of the succession are the result of in situ weathered bedrock (Chang, 1955; Ho, 1988). That interpretation might be due to a different usage of the term "bedrock", which describes in general the underlying beds in the Taiwanese literature. Although the top sediment layers in the Miaoli Tableland are intensively weathered, the loose and not lithified lower sediment units appear unweathered, and the entire sedimentary succession comprises unconsolidated sediments.

The tableland segments are separated by ongoing fluvial incision and backward erosion. Their special layout and morphology follow the fluvial pattern of the respective river catchments, which is dendritic in the SH-II and ST and more parallel in the SH-I. The cross sections of the fluvial channels between the segments are V-shaped above and box-shaped below 150 m a.s.l., respectively. This altitude marks at present the point in the longitudinal river profile where the fluvial morphodynamic changes from linear incision to lateral erosion with gravel accumulation (Charlton, 2008) representing the alluvial plains (AL). The box-shaped valleys are developed in the catchments with the dendritic drainage pattern. The formation of this pattern is supported by the fact that the lithology is basically consistent within the whole study area; thus the flow paths have developed freely, and they are not constrained by the geological or tectonic factors (e.g. the Tungxiao Anticline).

Integrating the results of this study into previous concepts (Chang et al., 1998; Ota et al., 2006), the landscape evolution of the Miaoli Tableland can be summarized as follows:

- Tidal and coastal sediments were deposited in the mountain foreland during periods of different but generally high sea levels in the Taiwan Strait. They are visible as the fine-grained sediments in the present ST and SH-II areas. These sediments represent the bay sediments in the interpretation of Chang et al. (1998). Whether they were also deposited in the present SH-I area is unknown.

- Subsequently, gravels and cobbles were deposited in the foreland basin in the form of one or several alluvial fans, which made up the present SH-I. Chang et al. (1998) suggested that they covered parts of the coastal sediments in the SH-II area. If they were transported by a single event or by multiple independent events by the Daan River, Wumei (Xihu) River, and Houlong River is also unknown. The terrain of the SH-I was subsequently uplifted along the Tongluo Fault (Ota et al., 2006), and thus the alluvial fans were prevented from further gravel and cobble accumulation.

- The ongoing uplift and the simultaneous incision of the SH-I induced the remobilization of the gravels and cobbles which were transported into the western and northern foreland of the SH-I, where they are accumulated as the present gravel and cobble layers of the SH-II and the ST. Further uplift of the SH-I along the present escarpment between the SH-I and the ST, which was assumed to be an inferred thrust fault (Chang et al., 1998), separated both terrains, stopped the gravel and cobble transport into the ST, and beheaded the valleys of the SH-I. The sediments in the ST area were slightly folded along the Tungxiao Anticline (Ota et al., 2006) during this terrain uplift. The folding may have enhanced the subsequent incision of the ST, where backward erosion is continuing in the upper and steeper channel sections. In this way, the gravels and cobbles are reworked again – from the ST surface into the AL channels and the (coastal) distal-tableland surfaces.

- The result of the rework is a cascade of gravel and cobble transportation in the Miaoli Tableland: previously from the mountains to the Sedimentary Highlands, then to the Sedimentary Terraces, and recently to the Alluvial and the Coastal Plains.

6 Conclusion

This study gives new detailed insights into the surface morphology and the sedimentary sequences of the Miaoli Tableland. The new high-resolution mapping enables the reconstruction of the palaeotopography of the region. The presented classification of tableland segments is thereby inferred from a mathematical calculation and widely independent from a subjective interpretation.

From the newly reconstructed palaeosurfaces in the western and northern part of the tableland we concluded that a quasi-continuous gravel and cobble cover existed not only in the Sedimentary Highlands but also in the Sedimentary Terraces, which is new in comparison with previous interpreta-

tions (Chang et al., 1998; Ota et al., 2006). This means that the Sedimentary Terraces (ST) and the northern Sedimentary Highlands (SH-II) covered originally a wider area than previously mapped (Chang et al., 1998). Our interpretation of cascade-like gravel and cobble rework implies that the main mass of gravels and cobbles was deposited originally in the southern Sedimentary Highlands (SH-I) and was reworked from there to the northern Sedimentary Highlands (SH-II) and the Sedimentary Terraces (ST).

Our sedimentological results suggest that the concept of the Lungkang Formation (Lin, 1963) or the Tûsyô/Tungxiao Formation (Chang, 1948; Makiyama, 1934, 1937) may be considered adequate stratigraphic terms to describe the tidal–fluvial–aeolian sediment succession of the uppermost 50–100 m in the northern and western part (SH-II and ST) of the Miaoli Tableland. Although absolute dating results are not available at this stage of research, the succession may represent one sedimentation cycle, which can be tentatively correlated with the last glacial cycle. Subsequent uplift brought the terrestrial sediments into a position above the Holocene sea-level high stand, provoking incision. The overall tableland morphology exhibits a stepwise sequence of sedimentation, uplift, and erosion in the area.

Fluvial incision created a characteristic drainage network with different patterns, depending on topographical parameters like the altitude and the location in the respective tableland areas but widely independent from the lithology in the Miaoli Tableland. The loose and easily erodible sediments enabled the formation of wide valley cross sections in the alluvial plains, which we tentatively named box-shaped valleys.

This study of terrace landforms in the frontal part of the mountain foreland in Taiwan has highlighted the possibility that a systematical terrain and sediment analysis can reveal new insights into the differentiated landform evolution in the Taiwanese foothills in the future.

Appendix A: Field photos of the Miaoli Tableland

Figure A1. Overview on the Tungxiao River catchment (the ST area) seen from the SH-I terrace (location: 24°26′57.92″ N, 120°45′15.42″ E; facing northwest, 24 October 2018). The tableland segments are dissected by channels of the dendritic fluvial network, visible in the centre of the photo.

Figure A2. Example of type I succession in outcrop 001_HLPT (location: 24°35′45.30″ N, 120°48′24.01″ E; facing west, 3 April 2015). The outcrop is about 49 m high and located on the left bank of the Houlong River. It shows fine-grained coastal sediments in the lower and central part and fluvial gravels and cobbles in the upper part.

Figure A3. Example of type II succession in outcrop 022_ZG (location: 24°28′55.02″ N, 120°42′8.09″ E; facing west, 8 January 2017). The outcrop is about 20 m high and located in the Tungxiao River catchment. It is excavated by a small creak, which is located between the outcrop and the road in the foreground. It represents the remnant of a tableland segment with fine-grained coastal sediments (greyish sand in the lower part and brownish sand in the upper part). The succession is covered by the silty cover layer (SiL) directly. This cover layer is barely visible between the vegetation in the upper central part of the picture.

Figure A4. Panorama photo of an example of type III succession in outcrop 051_LK (location: 24°36′37.61″ N, 120°44′52.69″ E; facing southeast, 23 October 2018). The outcrop is about 9 m high and located at the coast between the estuaries of the Houlong River and the Wumei (Xihu) River. It represents the sedimentary succession of the distal-tableland segments as part of the SH-II. The outcrop shows fine-grained sandy sediments covered by gravels and cobbles and modern aeolian sand. The gravels and cobbles appear as a channel infill in the centre of the picture.

Figure A5. A modernized channel in the box-shaped valley in the Tungxiao River catchment (location: 24°27′20.90″ N, 120°44′6.72″ E; facing west, 25 December 2014). The tableland segments in the background of this photo are classified as the ST. The valley floor is classified as AL; the fluvial channel is constrained by the artificial levees and covered by abundant gravel and cobble depositions.

Appendix B: Grain size distribution curves of all the studied samples

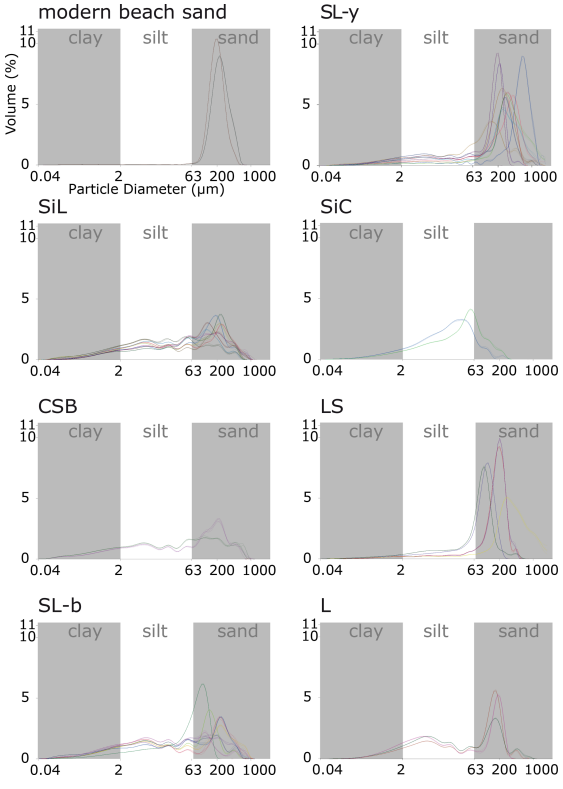

Figure B1. Samples are subgrouped by the corresponding sedimentary layers. Two samples are taken from the modern beach (dune) sand for comparison with the sandy materials in other layers. The grain size fractions are after the Wentworth scale.

Appendix C: Columnar sections and pictures of the outcrops in the Miaoli Tableland

See supplementary data of file 001-HLPT to 057-CTK at https://doi.org/10.17169/refubium-31813 (Liu et al., 2021).

Data availability. All relevant data used in this study are cited and presented in the text. Supplementary data of file 001-HLPT to 057-CTK are available at https://doi.org/10.17169/refubium-31813 (Liu et al., 2021).

Author contributions. All authors, SHL, RH, and MB, carried out the conceptualization, methodology, and investigation of this study together. SHL completed the fieldwork and the software and formal analyses, which are in the context of a PhD study programme supervised by MB. SHL and RH carried out the data visualization. This paper was drafted by SHL and revised by RH and MB.

Competing interests. Margot Böse is currently a member of the advisory board of *E&G Quaternary Science Journal*.

Disclaimer. Publisher's note: Copernicus Publications remains neutral with regard to jurisdictional claims in published maps and institutional affiliations.

Acknowledgements. The authors thank Jiun-Chuan Lin, Chia-Han Tseng, and Chia-Hung Jen for their friendly support of the fieldwork and Manfred Frechen for providing the access to the sediment lab. Moreover, we would like to thank Yu-Jia Chiu for the technical support of the base maps in Taiwan. Thanks go to Yan Li and Dirk Wenske for the discussion on the relevant topics and Christopher Lüthgens for the comments during the field observations. Thanks go to Shyh-Jeng Chyi and Lih-Der Ho for the comments during the INQUA Congress 2019. Thanks go to the Jing-Ji company and Chang Chun Petrochemical Co., Ltd Miaoli factory for the assessment of the outcrops. Finally, special thanks go to Li-Chun Xiao for managing the legal issues of open-access data usage for this study and Chu-Pan Lin for supporting the fieldwork.

Financial support. We acknowledge support from the Open Access Publication Initiative of Freie Universität Berlin.

Review statement. This paper was edited by Tony Reimann and reviewed by Toru Tamura and one anonymous referee.

References

Angelier, J., Barrier, E., and Chu, H. T.: Plate collision and paleostress trajectories in a fold-thrust belt: The foothills of Taiwan, Tectonophysics, 125, 161–178, https://doi.org/10.1016/0040-1951(86)90012-0, 1986.

Beuselinck, L., Govers, G., Poesen, J., Degraer, G., and Froyen, L.: Grain-size analysis by laser diffractometry: comparison with the sieve-pipette method, Catena, 32, 193–208, https://doi.org/10.1016/S0341-8162(98)00051-4, 1998.

Bridgland, D. and Westaway, R.: Climatically controlled river terrace staircases: A worldwide Quaternary phenomenon, Geomorphology, 98, 285–315, https://doi.org/10.1016/j.geomorph.2006.12.032, 2008.

Buatois, L. A., Santiago, N., Herrera, M., Plink-Björklund, P., Steel, R. O. N., Espin, M., and Parra, K.: Sedimentological and ichnological signatures of changes in wave, river and tidal influence along a Neogene tropical deltaic shoreline, Sedimentology, 59, 1568–1612, https://doi.org/10.1111/j.1365-3091.2011.01317.x, 2012.

Center for GIS RCHSS Academia Sinica: Taiwan Historical Atlas Web Map Tile Service [data set], available at: http://gis.sinica.edu.tw/tileserver/wmts (last access: 14 January 2022), 2017.

Central Geological Survey: National Geological Data Warehouse [data set], available at: https://gis3.moeacgs.gov.tw/gwh/gsb97-1/sys8/t3/index1.cfm (last access: 14 January 2022), 2017.

Central Weather Bureau: Typhoon Data Base [data set], available at: https://rdc28.cwb.gov.tw/TDB/ (last access: 14 January 2022), 2019.

Central Weather Bureau: Tidal level statistics [data set], available at: https://www.cwb.gov.tw/V8/C/C/MMC_STAT/sta_tide.html (last access: 14 January 2022), 2020.

Chang, H.-C.: Baishatun, Central Geological Survey, Geological Map of Taiwan scale 1 : 50 000, Taipei, Taiwan, available at: https://twgeoref.moeacgs.gov.tw/GipOpenWeb/wSite/ct?xItem=118492&ctNode=1303&mp=6 (last access: 14 January 2022), 1990.

Chang, H.-C.: Dajia, Central Geological Survey, Geological Map of Taiwan scale 1 : 50 000, Taipei, Taiwan, available at: https://twgeoref.moeacgs.gov.tw/GipOpenWeb/wSite/ct?xItem=118453&ctNode=333&mp=106 (last access: 14 January 2022), 1994.

Chang, J.-C., Teng, K.-H., and Liu, M.-C.: A Geomorphological Study on River Terraces in Miaoli Hills, Geogr. Res., 29, 97–112, https://doi.org/10.6234/JGR, 1998.

Chang, L.-S.: The revision of stratigraphy categories of Taiwan (continued), Geological Review, 13, 291–310, 1948.

Chang, L.-S.: Geologic map of Taiwan, Geological Survey of Taiwan, Taipei, Taiwan, available at: https://twgeoref.moeacgs.gov.tw/GipOpenWeb/wSite/ct?xItem=111421&ctNode=217&mp=6 (last access: 14 January 2022), 1953.

Chang, L.-S.: The strata of Taiwan, Quarterly Journal of the Taiwan Bank, 7, 26–49, 1955.

Charlton, R.: Fundamentals of fluvial geomorphology, Routledge, New York, USA, https://doi.org/10.4324/9780203371084, 2008.

Chen, C.-G.: Miaoli County, The soil investigation report of the slopes, Mountain Agricultural Resources Development Bureau,

Nantou, Taiwan, available at: https://tssurgo.tari.gov.tw/Tssurgo (last access: 14 January 2022), 1983.

Chen, H.-F., Yeh, P.-Y., Song, S.-R., Hsu, S.-C., Yang, T.-N., Wang, Y., Chi, Z., Lee, T.-Q., Chen, M.-T., Cheng, C.-L., Zou, J., and Chang, Y.-P.: The Ti/Al molar ratio as a new proxy for tracing sediment transportation processes and its application in aeolian events and sea level change in East Asia, J. Asian Earth Sci., 73, 31–38, https://doi.org/10.1016/j.jseaes.2013.04.017, 2013.

Chen, S., Steel, R. J., Dixon, J. F., and Osman, A.: Facies and architecture of a tide-dominated segment of the Late Pliocene Orinoco Delta (Morne L'Enfer Formation) SW Trinidad, Mar. Petrol. Geol., 57, 208–232, https://doi.org/10.1016/j.marpetgeo.2014.05.014, 2014.

Chen, W.-S., Ridgway, K. D., Horng, C.-S., Chen, Y.-G., Shea, K.-S., and Yeh, M.-G.: Stratigraphic architecture, magnetostratigraphy, and incised-valley systems of the Pliocene-Pleistocene collisional marine foreland basin of Taiwan, GSA Bulletin, 113, 1249–1271, https://doi.org/10.1130/0016-7606(2001)113<1249:SAMAIV>2.0.CO;2, 2001.

Chen, W.-S., Chen, Y.-G., Shih, R.-C., Liu, T.-K., Huang, N.-W., Lin, C.-C., Sung, S.-H., and Lee, K.-J.: Thrust-related river terrace development in relation to the 1999 Chi-Chi earthquake rupture, Western Foothills, central Taiwan, J. Asian Earth Sci., 21, 473–480, https://doi.org/10.1016/S1367-9120(02)00072-X, 2003.

Chen, Y.-G. and Liu, T.-K.: Sea Level Changes in the Last Several Thousand Years, Penghu Islands, Taiwan Strait, Quaternary Res., 45, 254–262, https://doi.org/10.1006/qres.1996.0026, 1996.

Chen, Y.-G., Shyu, J. B. H., Ota, Y., Chen, W.-S., Hu, J.-C., Tsai, B.-W., and Wang, Y.: Active structures as deduced from geomorphic features: a case in Hsinchu Area, northwestern Taiwan, Quaternary Int., 115–116, 189-199, https://doi.org/10.1016/s1040-6182(03)00107-1, 2004.

Chen, Z.-S., Hseu, Z.-Y., and Tsai, C.-C.: The soils of Taiwan, World soils book series, Springer, Dordrecht, https://doi.org/10.1007/978-94-017-9726-9, 2015.

Ching, K.-E., Hsieh, M.-L., Johnson, K. M., Chen, K.-H., Rau, R.-J., and Yang, M.: Modern vertical deformation rates and mountain building in Taiwan from precise leveling and continuous GPS observations, 2000–2008, J. Geophys. Res., 116, B08406, https://doi.org/10.1029/2011jb008242, 2011.

Choi, J. H., Kim, J. W., Murray, A. S., Hong, D. G., Chang, H. W., and Cheong, C.-S.: OSL dating of marine terrace sediments on the southeastern coast of Korea with implications for Quaternary tectonics, Quatern. Int., 199, 3–14, https://doi.org/10.1016/j.quaint.2008.07.009, 2009.

Covey, M.: The Evolution of Foreland Basins to Steady State: Evidence from the Western Taiwan Foreland Basin, in: Foreland Basins, Blackwell Publishing Ltd., 77–90, https://doi.org/10.1002/9781444303810.ch4, 1986.

Dadson, S. J., Hovius, N., Chen, H., Dade, W. B., Hsieh, M.-L., Willett, S. D., Hu, J.-C., Horng, M.-J., Chen, M.-C., Stark, C. P., Lague, D., and Lin, J.-C.: Links between erosion, runoff variability and seismicity in the Taiwan orogen, Nature, 426, 648–651, https://doi.org/10.1038/nature02150, 2003.

Dalrymple, R. W. and Choi, K.: Morphologic and facies trends through the fluvial–marine transition in tide-dominated depositional systems: A schematic framework for environmental and sequence-stratigraphic interpretation, Earth-Sci. Rev., 81, 135–174, https://doi.org/10.1016/j.earscirev.2006.10.002, 2007.

Davis, R. A.: Tidal Signatures and Their Preservation Potential in Stratigraphic Sequences, in: Principles of tidal sedimentology, edited by: Davis, R. A. and Dalrymple, R. W., Springer, Dordrecht, 35–55, https://doi.org/10.1007/978-94-007-0123-6_3, 2012.

Deffontaines, B., Lacombe, O., Angelier, J., Chu, H. T., Mouthereau, F., Lee, C. T., Deramond, J., Lee, J. F., Yu, M. S., and Liew, P. M.: Quaternary transfer faulting in the Taiwan Foothills: evidence from a multisource approach, Tectonophysics, 274, 61–82, https://doi.org/10.1016/S0040-1951(96)00298-3, 1997.

Delcaillau, B.: Geomorphic response to growing fault-related folds: example from the foothills of central Taiwan, Geodin. Acta, 14, 265–287, https://doi.org/10.1016/S0985-3111(01)01071-3, 2001.

Eshel, G., Levy, G. J., Mingelgrin, U., and Singer, M. J.: Critical Evaluation of the Use of Laser Diffraction for Particle-Size Distribution Analysis, Soil Sci. Soc. Am. J., 68, 736–743, https://doi.org/10.2136/sssaj2004.7360, 2004.

Goodbred, S. and Saito, Y.: Tide-Dominated Deltas, in: Principles of tidal sedimentology, edited by: Davis, R. A. and Dalrymple, R. W., Springer, Dordrecht, 129–149, https://doi.org/10.1007/978-94-007-0123-6_7, 2011.

Hanebuth, T. J. J., Voris, H. K., Yokoyama, Y., Saito, Y., and Okuno, J. I.: Formation and fate of sedimentary depocentres on Southeast Asia's Sunda Shelf over the past sea-level cycle and biogeographic implications, Earth-Sci. Rev., 104, 92–110, https://doi.org/10.1016/j.earscirev.2010.09.006, 2011.

Hebenstreit, R. and Böse, M.: Quaternary mineral aeolian dust deposits in Taiwan and their potentials as a new archive, XIX INQUA Congress, 27 July–2 August 2015, Nagoya, Japan, available at: https://www.inqua-seqs.org/files/INQUA2015_program_web.pdf (last access: 14 January 2022), 2015.

Ho, C.-S.: An introduction to the geology of Taiwan: explanatory text of the geologic map of Taiwan, Central Geological Survey, Taipei, Taiwan, available at: https://twgeoref.moeacgs.gov.tw/GipOpenWeb/wSite/ct?xItem=109139&ctNode=1303&mp=6 (last access: 14 January 2022), 1988.

Ho, H.-C.: Miaoli, Central Geological Survey, Geological Map of Taiwan scale 1 : 50 000, Taipei, Taiwan, available at: https://twgeoref.moeacgs.gov.tw/GipOpenWeb/wSite/ct?xItem=118489&ctNode=1303&mp=6 (last access: 14 January 2022), 1994.

Horng, C.-S.: Age of the Tananwan Formation in Northern Taiwan: A Reexamination of the Magnetostratigraphy and Calcareous Nannofossil Biostratigraphy, Terr. Atmos. Ocean. Sci., 25, 137–147, https://doi.org/10.3319/tao.2013.11.05.01(tt), 2014.

Horng, C.-S. and Huh, C.-A.: Magnetic properties as tracers for source-to-sink dispersal of sediments: A case study in the Taiwan Strait, Earth Planet. Sc. Lett., 309, 141–152, https://doi.org/10.1016/j.epsl.2011.07.002, 2011.

Huang, T.: Planktic foraminiferal biostratigraphy and datum planes in the Neogene sedimentary sequence in Taiwan, Palaeogeogr. Palaeocl., 46, 97–106, https://doi.org/10.1016/0031-0182(84)90028-2, 1984.

Huh, C.-A., Chen, W., Hsu, F.-H., Su, C.-C., Chiu, J.-K., Lin, S., Liu, C.-S., and Huang, B.-J.: Modern (< 100 years) sedimentation in the Taiwan Strait: Rates and source-to-sink pathways elucidated from radionuclides and particle size distribution, Cont. Shelf Res., 31, 47–63, https://doi.org/10.1016/j.csr.2010.11.002, 2011.

Jahn, R., Blume, H. P., Asio, V. B., Spaargaren, O., and Schad, P.: Guidelines for soil description, 4th edn., Food and Agriculture Organization of the United Nations, Rome, ISBN 9251055211, 2006.

Jan, S., Wang, J., Chern, C.-S., and Chao, S.-Y.: Seasonal variation of the circulation in the Taiwan Strait, J. Marine Syst., 35, 249–268, https://doi.org/10.1016/S0924-7963(02)00130-6, 2002.

Konert, M. and Vandenberghe, J.: Comparison of laser grain size analysis with pipette and sieve analysis: a solution for the underestimation of the clay fraction, Sedimentology, 44, 523–535, https://doi.org/10.1046/j.1365-3091.1997.d01-38.x, 1997.

Lee, C.-L., Huang, T., Shieh, K.-S., and Chen, Z.-H.: The chronostratigraphy and sedimentary environments of the Toukoshan Fm. in Beishatun area, Miaoli, Annual Report of Central Geological Survey, MOEA, 1999–2000, 17–20, available at: https://twgeoref.moeacgs.gov.tw/GipOpenWeb/wSite/ct?xItem=111058&ctNode=1303&mp=6 (last access: 14 January 2022), 2002.

Lee, J.-F.: Dongshi, Central Geological Survey, Geological Map of Taiwan scale 1 : 50 000, Taipei, Taiwan, available at: https://twgeoref.moeacgs.gov.tw/GipOpenWeb/wSite/ct?xItem=118454&ctNode=1303&mp=6 (last access: 14 January 2022), 2000.

Lin, A. T. and Watts, A. B.: Origin of the West Taiwan basin by orogenic loading and flexure of a rifted continental margin, J. Geophys. Res.-Sol. Ea., 107, ETG 2-1–ETG 2-19, https://doi.org/10.1029/2001jb000669, 2002.

Lin, A. T., Watts, A. B., and Hesselbo, S. P.: Cenozoic stratigraphy and subsidence history of the South China Sea margin in the Taiwan region, Basin Res., 15, 453–478, https://doi.org/10.1046/j.1365-2117.2003.00215.x, 2003.

Lin, C. C.: Geomorphology of Taiwan, The Historical Research Commission of Taiwan Province, Taipei, Taiwan, 1957.

Lin, C. C.: The Lungkang Formation, lower marine terrace deposits near Miaoli, Petroleum Geology of Taiwan, 2, 87–105, 1963.

Lin, C. C.: Holocene Geology of Taiwan, Acta Geologica Taiwanica, 13, 83–126, 1969.

Lin, C. C. and Chou, J. T.: Geology of Taiwan, Maw Chang Book Co., Ltd., Taipei, Taiwan, 1978.

Liu, J. P., Milliman, J. D., Gao, S., and Cheng, P.: Holocene development of the Yellow River's subaqueous delta, North Yellow Sea, Mar. Geol., 209, 45–67, https://doi.org/10.1016/j.margeo.2004.06.009, 2004.

Liu, J. P., Liu, C. S., Xu, K. H., Milliman, J. D., Chiu, J. K., Kao, S. J., and Lin, S. W.: Flux and fate of small mountainous rivers derived sediments into the Taiwan Strait, Mar. Geol., 256, 65–76, https://doi.org/10.1016/j.margeo.2008.09.007, 2008.

Liu, S.-H., Böse, M., and Hebenstreit, R.: The columnar sections and pictures of the outcrops in Miaoli Tableland, Refubium – Freie Universität Berlin Repository [data set], https://doi.org/10.17169/refubium-31813, 2021.

Makiyama, T.: Hakusyaton Sheet, Bureau of Productive Industries, Government-General of Taiwan, Explanatory text of the geological map of Taiwan (1 : 50 000), Tokyo, Japan, available at: https://twgeoref.moeacgs.gov.tw/GipOpenWeb/wSite/ct?xItem=119130&ctNode=217&mp=6 (last access: 14 January 2022), 1934.

Makiyama, T.: The topographic and geological map of Tûsyô petroleum field, Bureau of Productive Industries, Government-General of Taiwan, Tokyo, Japan, available at: https://twgeoref.moeacgs.gov.tw/GipOpenWeb/wSite/ct?xItem=108126&ctNode=1304&mp=104 (last access: 14 January 2022), 1937.

Mather, A. E., Stokes, M., and Whitfield, E.: River terraces and alluvial fans: The case for an integrated Quaternary fluvial archive, Quaternary Sci. Rev., 166, 74–90, https://doi.org/10.1016/j.quascirev.2016.09.022, 2017.

Matsu'ura, T., Kimura, H., Komatsubara, J., Goto, N., Yanagida, N., Ichikawa, K., and Furusawa, A.: Late Quaternary uplift rate inferred from marine terraces, Shimoka Peninsula, northeastern Japan: A preliminary investigation of the buried shoreline angle, Geomorphology, 209, 1–17, https://doi.org/10.1016/j.geomorph.2013.11.013, 2014.

Miall, A. D.: Fluvial Depositional Systems, Springer Geology, Springer International Publishing, Switzerland, 316 pp., https://doi.org/10.1007/978-3-319-24304-7, 2014.

NASA JPL: 1 Arc Second scene N24 E120 [data set], https://doi.org/10.5067/MEaSUREs/SRTM/SRTMGL1.003, 2013.

National Land Surveying and Mapping Center: Taiwan Map Service [data set], available at: https://wmts.nlsc.gov.tw/wmts (last access: 14 January 2022), 2016.

Olariu, C., Steel, R. J., Dalrymple, R. W., and Gingras, M. K.: Tidal dunes versus tidal bars: The sedimentological and architectural characteristics of compound dunes in a tidal seaway, the lower Baronia Sandstone (Lower Eocene), Ager Basin, Spain, Sediment. Geol., 279, 134–155, https://doi.org/10.1016/j.sedgeo.2012.07.018, 2012.

Ota, Y., Shyu, J. B., Chen, Y.-G., and Hsieh, M.-L.: Deformation and age of fluvial terraces south of the Choushui River, central Taiwan, and their tectonic implications, Western Pacific Earth Sciences, 2, 251–260, 2002.

Ota, Y., Chen, Y.-G., and Chen, W.-S.: Review of paleoseismological and active fault studies in Taiwan in the light of the Chichi earthquake of September 21, 1999, Tectonophysics, 408, 63–77, https://doi.org/10.1016/j.tecto.2005.05.040, 2005.

Ota, Y., Lin, Y.-N. N., Chen, Y.-G., Chang, H.-C., and Hung, J.-H.: Newly found Tunglo Active Fault System in the fold and thrust belt in northwestern Taiwan deduced from deformed terraces and its tectonic significance, Tectonophysics, 417, 305–323, https://doi.org/10.1016/j.tecto.2006.02.001, 2006.

Ota, Y., Lin, Y.-N. N., Chen, Y.-G., Matsuta, N., Watanuki, T., and Chen, Y.-W.: Touhuanping Fault, an active wrench fault within fold-and-thrust belt in northwestern Taiwan, documented by spatial analysis of fluvial terraces, Tectonophysics, 474, 559–570, https://doi.org/10.1016/j.tecto.2009.04.034, 2009.

Pelletier, B. and Stephan, J. F.: Middle miocene deduction and late miocene beginning of collision registered in the hengchun peninsula: Geodynamic implications for the evolution of Taiwan, Tectonophysics, 125, 133–160, https://doi.org/10.1016/0040-1951(86)90011-9, 1986.

Pickering, J. L., Goodbred, S. L., Reitz, M. D., Hartzog, T. R., Mondal, D. R., and Hossain, M. S.: Late Quaternary sedimentary record and Holocene channel avulsions of the Jamuna and Old Brahmaputra River valleys in the upper Bengal delta plain, Geomorphology, 227, 123–136, https://doi.org/10.1016/j.geomorph.2013.09.021, 2014.

Pye, K. and Zhou, L.-P.: Late Pleistocene and Holocene aeolian dust deposition in North China and the Northwest Pacific Ocean, Palaeogeogr. Palaeocl., 73, 11–23, https://doi.org/10.1016/0031-0182(89)90041-2, 1989.

Robustelli, G., Ermolli, E. R., Petrosino, P., Jicha, B., Sardella, R., and Donato, P.: Tectonic and climatic control on geomorphological and sedimentary evolution of the Mercure basin, southern Apennines, Italy, Geomorphology, 214, 423–435, https://doi.org/10.1016/j.geomorph.2014.02.026, 2014.

Saito, K. and Oguchi, T.: Slope of alluvial fans in humid regions of Japan, Taiwan and the Philippines, Geomorphology, 70, 147–162, https://doi.org/10.1016/j.geomorph.2005.04.006, 2005.

Satellite Survey Center: Ministry of the Interior 20 m raster digital elevation model [data set], available at: https://data.gov.tw/dataset/35430 (last access: 14 January 2022), 2018.

Shackleton, N. J.: The 100,000-Year Ice-Age Cycle Identified and Found to Lag Temperature, Carbon Dioxide, and Orbital Eccentricity, Science, 289, 1897–1902, https://doi.org/10.1126/science.289.5486.1897, 2000.

Shih, T.-T. and Yang, G.-S.: The Active Faults and Geomorphic Surfaces of Pakua Tableland in Taiwan, Geogr. Res., 11, 173–186, 1985.

Shyu, J. B. H., Sieh, K., Chen, Y.-G., and Liu, C.-S.: Neotectonic architecture of Taiwan and its implications for future large earthquakes, J. Geophys. Res., 110, B08402, https://doi.org/10.1029/2004jb003251, 2005.

Siame, L. L., Chen, R.-F., Derrieux, F., Lee, J.-C., Chang, K.-J., Bourlès, D. L., Braucher, R., Léanni, L., Kang, C.-C., Chang, C.-P., and Chu, H.-T.: Pleistocene alluvial deposits dating along frontal thrust of Changhua Fault in western Taiwan: The cosmic ray exposure point of view, J. Asian Earth Sci., 51, 1–20, https://doi.org/10.1016/j.jseaes.2012.02.002, 2012.

Simoes, M. and Avouac, J. P.: Investigating the kinematics of mountain building in Taiwan from the spatiotemporal evolution of the foreland basin and western foothills, J. Geophys. Res., 111, B10401, https://doi.org/10.1029/2005jb004209, 2006.

Suppe, J.: Kinematics of arc-continent collision, flipping of subduction, and back-arc spreading near Taiwan, Memoir of the Geological Society of China, 6, 131–146, 1984.

Teng, K.-H.: A Quantitative Study on the Landforms of Lateritic Gravel Tablelands in Northwestern Taiwan, The College of Chinese Culture Institute of Geography Science Reports, 3, 113–186, 1979.

Teng, L. S.: Geotectonic evolution of late Cenozoic arc-continent collision in Taiwan, Tectonophysics, 183, 57–76, https://doi.org/10.1016/0040-1951(90)90188-E, 1990.

Teng, L.-S.: Geotectonic evolution of Tertiary continental margin basins of Taiwan, Petroleum Geology of Taiwan, 27, 1–19, 1992.

Teng, L. S.: Extensional collapse of the northern Taiwan mountain belt, Geology, 24, 949–952, 1996a.

Teng, L. S.: Geological background of the gravel formations of Taiwan, Sine-Geotechnics, 55, 5–24, https://doi.org/10.30140/SG.199606.0001, 1996b.

Teng, L. S., Lee, C., Peng, C.-H., Chen, W.-F., and Chu, C.-J.: Origin and geological evolution of the Taipei basin, northern Taiwan, Western Pacific Earth Sciences, 1, 115–142, 2001.

The Taiwan Provincial Weather Institution: Report on Floods of 7th August, 1959, The Taiwan Provincial Weather Institution, Taipei, Taiwan, available at: https://photino.cwb.gov.tw/rdcweb/lib/cd/cd02tyrp/typ/1959/6.pdf (last access: 14 January 2022), 1959.

Tomita, Y.: On the geomorphological classification of fans in Taiwan (Formosa), Journal of Geography (Chigaku Zasshi), 60, 2–9, 1951.

Tomita, Y.: The classification of fluvial terraces, Annals of The Tohoku Geographycal Asocciation, 6, 1–6, https://doi.org/10.5190/tga1948.6.1, 1953.

Tomita, Y.: Surface Geology and Correlation of River Terraces, Annals of The Tohoku Geographycal Asocciation, 6, 51–58, https://doi.org/10.5190/tga1948.6.4_51, 1954.

Torii, K.: Tosei Sheet, Bureau of Productive Industries, Government-General of Taiwan, Explanatory text of the geological map of Taiwan (1 : 50 000), Tokyo, available at: https://twgeoref.moeacgs.gov.tw/GipOpenWeb/wSite/ct?xItem=104094&ctNode=217&mp=6 (last access: 14 January 2022), 1935.

Tsai, H., Huang, W.-S., Hseu, Z.-Y., and Chen, Z.-S.: A River Terrace Soil Chronosequence of the Pakua Tableland in Central Taiwan, Soil Science, 171, 167–179, https://doi.org/10.1097/01.ss.0000187376.76767.21, 2006.

Tsai, H., Maejima, Y., and Hseu, Z.-Y.: Meteoric 10Be dating of highly weathered soils from fluvial terraces in Taiwan, Quaternary Int., 188, 185–196, https://doi.org/10.1016/j.quaint.2007.06.007, 2008.

Tsai, H., Hseu, Z.-Y., Huang, S.-T., Huang, W.-S., and Chen, Z.-S.: Pedogenic properties of surface deposits used as evidence for the type of landform formation of the Tadu tableland in central Taiwan, Geomorphology, 114, 590–600, https://doi.org/10.1016/j.geomorph.2009.09.020, 2010.

Tseng, C.-H., Wenske, D., Böse, M., Reimann, T., Lüthgens, C., and Frechen, M.: Sedimentary features and ages of fluvial terraces and their implications for geomorphic evolution of the Taomi River catchment: A case study in the Puli Basin, central Taiwan, J. Asian Earth Sci., 62, 759–768, https://doi.org/10.1016/j.jseaes.2012.11.028, 2013.

Vail, P. R., Audemade, F., Bowman, S. A., Eisner, P. N., and Perez-Cruz, C.: The stratigraphic signatures of tectonics, eustacy and sedimentology – an overview, in: Cycles and Events in Stratigraphy, edited by: Einsele, G., Ricken, W., and Seilacher, A., Springer-Verlag, Berlin, 617–659, ISBN 3540527842, 1991.

Volker, H. X., Wasklewicz, T. A., and Ellis, M. A.: A topographic fingerprint to distinguish alluvial fan formative processes, Geomorphology, 88, 34–45, https://doi.org/10.1016/j.geomorph.2006.10.008, 2007.

Wang, Y. H., Jan, S., and Wang, D. P.: Transports and tidal current estimates in the Taiwan Strait from shipboard ADCP observations (1999–2001), Estuar., Coast. Shelf Sci., 57, 193–199, https://doi.org/10.1016/S0272-7714(02)00344-X, 2003.

Willemin, J. H. and Knuepfer, P. L. K.: Kinematics of arc-continent collision in the eastern Central Range of Taiwan inferred from geomorphic analysis, J. Geophys. Res.-Sol. Ea., 99, 20267–20280, https://doi.org/10.1029/94JB00731, 1994.

Yang, K.-M., Huang, S.-T., Wu, J.-C., Ting, H.-H., and Mei, W.-W.: Review and New Insights on Foreland Tectonics in Western Taiwan, Int. Geol. Rev., 48, 910–941, https://doi.org/10.2747/0020-6814.48.10.910, 2006.

Yang, K.-M., Huang, S.-T., Jong-Chang, W., Ting, H.-H., Wen-Wei, M., Lee, M., Hsu, H.-H., and Lee, C.-J.: 3D geometry of the Chelungpu thrust system in central Taiwan: Its implications for active tectonics, Terr. Atmos. Ocean. Sci., 18, 143, https://doi.org/10.3319/TAO.2007.18.2.143(TCDP), 2007.

Yang, K.-M., Rau, R.-J., Chang, H.-Y., Hsieh, C.-Y., Ting, H.-H., Huang, S.-T., Wu, J.-C., and Tang, Y.-J.: The role of basement-involved normal faults in the recent tectonics of western Taiwan, Geol. Mag., 153, 1166–1191, https://doi.org/10.1017/S0016756816000637, 2016.

Yu, H.-S. and Chou, Y.-W.: Characteristics and development of the flexural forebulge and basal unconformity of Western Taiwan Foreland Basin, Tectonophysics, 333, 277–291, https://doi.org/10.1016/S0040-1951(00)00279-1, 2001.

Yu, H.-S. and Song, G. S.: Submarine physiographic features in Taiwan region and their geological significance, Journal of the Geological Society of China, 43, 267–286, 2000.

Yu, N.-T., Teng, L. S., Chen, W.-S., Yue, L.-F., and Chen, M.-M.: Early post-rift sequence stratigraphy of a Mid-Tertiary rift basin in Taiwan: Insights into a siliciclastic fill-up wedge, Sediment. Geol., 286–287, 39–57, https://doi.org/10.1016/j.sedgeo.2012.12.009, 2013.